Trans-generational transmission of environmental information in *C. elegans*

Adam Klosin[1,2], Eduard Casas[3], Cristina Hidalgo-Carcedo[1,2], Tanya Vavouri[3,4,*] and Ben Lehner[1,2,5,*]

[1]EMBL-CRG Systems Biology Unit, Centre for Genomic Regulation (CRG), 08003 Barcelona, Spain.

[2]Universitat Pompeu Fabra (UPF), 08003 Barcelona, Spain.

[3] Program for Predictive and Personalized Medicine of Cancer (PMPPC), Institute Germans Trias I Pujol (IGTP), Campus Can Ruti, Badalona 08916, Barcelona, Spain

[4]Josep Carreras Leukaemia Research Institute (IJC), Badalona 08916, Barcelona, Spain

[5]Institució Catalana de Recerca i Estudis Avançats (ICREA), 08010 Barcelona, Spain

*Correspondence: ben.lehner@crg.eu, tvavouri@carrerasresearch.org

Abstract

The environment experienced by an animal can sometimes influence gene expression for one or a few subsequent generations. Here we observe that a temperature-induced change in expression from a *C. elegans* heterochromatic gene array can endure for at least 14 generations. Inheritance is primarily in *cis* with the locus, occurs through both oocytes and sperm, and is associated with altered trimethylation of histone H3 lysine 9 (H3K9me3) before the onset of zygotic transcription. Expression profiling reveals that temperature-induced expression from endogenous repressed repeats can also be inherited for multiple generations. Long-lasting epigenetic memory of environmental change is therefore possible in this animal.

Main text

Resident animals are not the only ones subject to their environment, but their progeny can also be affected (*1-11*). For example, starvation or exposure to high temperature in *C. elegans* can lead to altered small RNA transmission and putative target mRNA expression for up to three generations (*12, 13*), and a few temperature-induced expression changes have been detected for two generations in animals with an inactive nuclear RNAi pathway (*14*). In contrast, gene silencing initiated by exogenous dsRNA or piRNAs can sometimes be stably inherited between generations (*15-19*).

When we subjected *C. elegans* to high temperature (25°C), expression from *daf-21 (Hsp90)* promoter::fluorescent protein constructs was strongly elevated (Figure S1). Expression from a single copy transgene was still elevated in the progeny of animals transferred from after five generations at 25°C to 20°C, but not in their descendants (Figure S1A). In contrast, expression from an integrated multi-copy array took fourteen generations to return to basal levels after the temperature was reduced after five generations at 25°C (Figure 1A, Figure S1). A single generation of growth at 25°C was sufficient to generate a seven-generation memory of increased expression (Figure S1C). Multi-generation inheritance of temperature-induced expression and transgene-dependent phenotypes was also observed with other high copy arrays (Table S1).

mRNA transcribed from a *daf-21* promoter array is first detected in wild-type (wt) worms at the 16-cell stage of development, confirming no maternal supply of mRNA to the embryo (Figure S2, (*20*)). Expression differences inherited from parents reared at different temperatures or sorted according to their expression were apparent from the onset of zygotic transcription (Figure 1B, Figure S3) and genetic crosses demonstrated inheritance through both oocytes (Figure 1C) and sperm (Figure 1D). The array is therefore inherited in an inactive state but poised for a specific level of activation that reflects expression in the previous generation.

To distinguish whether inheritance occurs in *cis* with the DNA locus or in *trans* – for example in the cytoplasm – we crossed worms with high and low expression to each other and then crossed the resulting F1 male progeny to wt hermaphrodites (Figure S4

(*20*)). The bimodal distribution of expression in the F2 progeny indicates that the major mode of inheritance is in *cis* with the locus (Figure 1E, (*21*)).

To investigate chromatin modifications as potential mediators of this inheritance, we quantified histone modifications on the array in early embryos developing at 20°C whose grandparents had developed at either 16°C or 25°C (Figure 2A). Embryos whose grandparents developed at 25°C had less of the repressive histone modification H3K9me3 on the array than embryos whose grandparents developed at 16°C (Figure 2A and B). This difference was apparent in early embryos before the onset of zygotic transcription, indicating that the altered chromatin is not a secondary response to altered transcription in the embryo (Figure 2A and B). No differences were observed in the Polycomb-associated repressive modification H3K27me3 or in H3K36me3 and H3K4me2, two modifications associated with active chromatin (Figure 2B, Figure S5). The differences in H3K9me3 were maintained in late embryos after the onset of transcription (Figure S6)

No mRNA expression from the array was detected in the adult germline (Figure S7). However, H3K9me3 was reduced on the array in the germline nuclei of adults that had been transferred from 16°C to 25°C as embryos (Figure 2C-D, Figure S8). Therefore, high temperature during germline development results in depletion of H3K9me3 from the array, even though there is no production of stable transcripts in this tissue.

The putative histone methyltransferase, SET-25, is responsible for all detectable H3K9me3 in *C. elegans* embryos (*22*) (Figure S5B), co-localizes with H3K9me3 enriched transgenic arrays within embryonic nuclei (*22*), and is required for the maintenance of piRNA-initiated stable gene silencing (*15*). Inactivating *set-25* increased expression from the array, with no difference in expression between animals maintained at 20 or 25 °C (Figure 3A-B). Hence, the repression of the array at low temperature requires SET-25. Moreover, no differences in expression were observed between the F1 offspring of *set-25* hermaphrodites mated with male animals transmitting an array with either high or low expression (Figure 3B). In contrast, the inactivation of seven other chromatin and small RNA pathway components (including a Polycomb mutant *mes-2*) showed no obvious defects in the transmission of the

expression memory (Figure S9). Even after >20 generations of growth at a constant temperature substantial variation in transgene expression is observed in both wt and *set-25* mutant populations (Figure 3C). In wt animals these differences are transmitted to the next generation (Figure 3C), but this is not the case in *set-25* mutants (Figure 3C).

Our results suggest a simple model for how the transgene array shows memory of high temperature exposure that endures for many generations (Figure S10). High temperature inhibits SET-25-mediated repression in the germline causing loss of H3K9me3 from the array. This de-repressed chromatin is transmitted to subsequent generations resulting in increased expression when transcription initiates in somatic lineages. Over multiple generations of growth at low temperature, repression is gradually restored by heterochromatin remodeling in each germline cycle. This is consistent with previously-reported gradual quantitative inter-generational changes in H3K9me3 following a temperature change at some loci (*14*).

We tested whether this model predicts the behavior of endogenous loci in the genome by sequencing RNA from *set-25* mutants and wt animals at 20°C and 25°C and three generations after a change from 25°C to 20°C. For protein-coding genes, de-repression in *set-25* mutants provided weak prediction of increased expression at high temperature (Figure S11), consistent with a larger contribution from other regulators such as specific transcription factors. De-repression in *set-25* mutants was, however, a better predictor of increased expression at high temperature for multiple classes of repetitive elements and also for pseudogenes (Figure 4A, Figure S11-14), consistent with impaired SET-25 activity making an important contribution to the increased expression of many loci at high temperature.

The increased expression of loci repressed by SET-25 with increased expression at high temperature was, although small, still detectable three generations after a return to low temperature (Figure 4A-B, Figure S11-14). Quantifying the expression of two DNA transposons by quantitative real-time PCR in independent samples confirmed that their expression remained elevated for four and five generations after a return to 20°C

(Figure 4C, Figure S15). Their expression was also confirmed as SET-25-dependent (Figure 4D).

Taken together, these results support the mechanistic model: at high temperature, SET-25 activity is reduced, resulting in the de-repression of many loci in the genome. After a return to low temperature, SET-25 activity is restored but it takes multiple generations for repression to be completely re-established. Expression from SET-25-repressed repeats therefore transmits information about a prior environmental exposure in this species.

In mammals, repressed repetitive elements can also escape epigenetic reprogramming (*23, 24*) with variation in the expression of both individual repeats (*25*) and multi-copy heterochromatic transgenes (*26*) being transmitted between generations. In flies, diet- (*6*) and stress-induced (*5*) changes in heterochromatin can also be transmitted for at least one generation. It is possible therefore that environmentally-triggered changes in heterochromatin may provide a general mechanism for the epigenetic transmission of information between generations. It is interesting to speculate that the inheritance of environmentally-triggered changes in expression from repressed chromatin may have been co-opted to provide adaptive benefits to an organism.

References and notes

1. J. C. Jimenez-Chillaron *et al.*, Intergenerational transmission of glucose intolerance and obesity by in utero undernutrition in mice. *Diabetes* **58**, 460-468 (2009).
2. J. J. Remy, Stable inheritance of an acquired behavior in Caenorhabditis elegans. *Current biology : CB* **20**, R877-878 (2010).
3. S. F. Ng *et al.*, Chronic high-fat diet in fathers programs beta-cell dysfunction in female rat offspring. *Nature* **467**, 963-966 (2010).
4. B. R. Carone *et al.*, Paternally induced transgenerational environmental reprogramming of metabolic gene expression in mammals. *Cell* **143**, 1084-1096 (2010).
5. K. H. Seong, D. Li, H. Shimizu, R. Nakamura, S. Ishii, Inheritance of stress-induced, ATF-2-dependent epigenetic change. *Cell* **145**, 1049-1061 (2011).
6. A. Ost *et al.*, Paternal diet defines offspring chromatin state and intergenerational obesity. *Cell* **159**, 1352-1364 (2014).
7. E. J. Radford *et al.*, In utero effects. In utero undernourishment perturbs the adult sperm methylome and intergenerational metabolism. *Science (New York, N.Y.)* **345**, 1255903 (2014).

8. D. Martinez *et al.*, In utero undernutrition in male mice programs liver lipid metabolism in the second-generation offspring involving altered Lxra DNA methylation. *Cell Metab* **19**, 941-951 (2014).
9. M. A. Jobson *et al.*, Transgenerational Effects of Early Life Starvation on Growth, Reproduction, and Stress Resistance in Caenorhabditis elegans. *Genetics* **201**, 201-212 (2015).
10. P. Huypens *et al.*, Epigenetic germline inheritance of diet-induced obesity and insulin resistance. *Nat Genet* **48**, 497-499 (2016).
11. A. Klosin, B. Lehner, Mechanisms, timescales and principles of trans-generational epigenetic inheritance in animals. *Current opinion in genetics & development* **36**, 41-49 (2016).
12. O. Rechavi *et al.*, Starvation-induced transgenerational inheritance of small RNAs in C. elegans. *Cell* **158**, 277-287 (2014).
13. D. Schott, I. Yanai, C. P. Hunter, Natural RNA interference directs a heritable response to the environment. *Scientific reports* **4**, 7387 (2014).
14. J. Z. Ni *et al.*, A transgenerational role of the germline nuclear RNAi pathway in repressing heat stress-induced transcriptional activation in C. elegans. *Epigenetics Chromatin* **9**, 3 (2016).
15. A. Ashe *et al.*, piRNAs can trigger a multigenerational epigenetic memory in the germline of C. elegans. *Cell* **150**, 88-99 (2012).
16. M. J. Luteijn *et al.*, Extremely stable Piwi-induced gene silencing in Caenorhabditis elegans. *The EMBO journal* **31**, 3422-3430 (2012).
17. M. Shirayama *et al.*, piRNAs initiate an epigenetic memory of nonself RNA in the C. elegans germline. *Cell* **150**, 65-77 (2012).
18. B. A. Buckley *et al.*, A nuclear Argonaute promotes multigenerational epigenetic inheritance and germline immortality. *Nature* **489**, 447-451 (2012).
19. S. G. Gu *et al.*, Amplification of siRNA in Caenorhabditis elegans generates a transgenerational sequence-targeted histone H3 lysine 9 methylation footprint. *Nat Genet* **44**, 157-164 (2012).
20. See supplementary materials on Science Online.
21. S. Berry, M. Hartley, T. S. Olsson, C. Dean, M. Howard, Local chromatin environment of a Polycomb target gene instructs its own epigenetic inheritance. *eLife* **4**, (2015).
22. B. D. Towbin *et al.*, Step-wise methylation of histone H3K9 positions heterochromatin at the nuclear periphery. *Cell* **150**, 934-947 (2012).
23. J. A. Hackett *et al.*, Germline DNA demethylation dynamics and imprint erasure through 5-hydroxymethylcytosine. *Science (New York, N.Y.)* **339**, 448-452 (2013).
24. W. W. Tang *et al.*, A Unique Gene Regulatory Network Resets the Human Germline Epigenome for Development. *Cell* **161**, 1453-1467 (2015).
25. H. D. Morgan, H. G. Sutherland, D. I. Martin, E. Whitelaw, Epigenetic inheritance at the agouti locus in the mouse. *Nat Genet* **23**, 314-318 (1999).
26. L. Daxinger, E. Whitelaw, Understanding transgenerational epigenetic inheritance via the gametes in mammals. *Nat Rev Genet* **13**, 153-162 (2012).

Acknowledgements

This work was supported by a European Research Council (ERC) Consolidator grant (616434), the Spanish Ministry of Economy and Competitiveness (BFU2011-26206 and SEV-2012-0208), the AXA Research Fund, the Bettencourt Schueller Foundation, Agencia de Gestio d'Ajuts Universitaris i de Recerca (AGAUR), FP7 project 4DCellFate (277899), and the EMBL-CRG Systems Biology Program. A.K. was partially supported by a la Caixa Fellowship. E.C and T.V. were supported by the Spanish Ministry of Economy and Competitiveness (BFU2015-70581) and by an FI AGAUR PhD fellowship to E.C. RNA-seq experiments were performed in the CRG Genomics core facility. RNA-seq datasets are deposited in the NCBI GEO under accession GSE83528.

List of Supplementary Materials

Materials and methods

Figs. S1-15

Tables S1-S4

References [9]

Figure legends

Figure 1. Fourteen generation memory of high temperature.

(A) Adult expression of a *daf-21p::mCHERRY* integrated multicopy transgene at 20 °C after five generations at 25 °C. Scale bar = 0.1 mm. Stage-matched worms at 20 °C used as a reference for normalization (black). False discovery rates (FDR) q-values: **** q< 0.0001, *** q<0.001, ** q<0.01, ns q> 0.05 (Wilcoxon test). Sample size indicated. (B) Expression in embryos from animals transferred to 20 °C at the L4 stage (inset: quantification at 500 mins). Arrowhead indicates start of zygotic transcription of the transgene. Transmission occurs through oocytes (C) and sperm (D) and in *cis* with the locus (E). See Figure S4 for design, intensities normalized to the 'low' population; sample size and p-value for Hartigans' dip test for unimodality.

Figure 2. Changes in H3K9me3.

(A-B) H3K9me3 is depleted from the transgene locus in the F2 descendants of animals grown at 25 °C. L4 larvae from populations grown at 16 °C and 25 °C were transferred to 20 °C and cultivated until the following F1 generation reached adulthood. The F2 embryos were extracted and histone modifications quantified on the array by immunofluorescence combined with DNA-FISH (A) Representative 2-cell stage embryos stained with DAPI (blue), anti-H3K9me3 (pink) and a DNA FISH probe complementary to mCHERRY (green). Arrows indicate transgene loci. See Figure S5. (B) Quantification of histone modifications in early embryos. (C-D) Development at high temperature from embryo to adult results in reduced H3K9me3 on the array in the germline nuclei of adults. Gonads were extracted from adult worms shifted from 16 to 25 °C during embryonic development, fixed, stained and compared to those from animals kept constantly at 16 °C. (C) Representative gonads stained with DAPI (blue), anti-H3K9me3 (pink) and a DNA FISH probe complementary to mCHERRY (green). (D) Each boxplot quantifies the nuclei of a single gonad (see also Figure S8).

Figure 3. Requirement for SET-25.

(A) Quantification of *daf-21p::mCHERRY* expression in L4 larvae at 20 and 25 °C in wt and *set-25* mutants. (B) Expression of a paternally-derived transgene in the adult progeny of wt and *set-25* mutant mothers. A common batch of low and (temperature-

induced) high expressing males was used. (C) Quantification of *daf-21p::mCHERRY* expression in the self-progeny (F1) of animals sorted into 'high' and 'low' groups (P0) based on transgene expression in wt and *set-25* mutants. Scale bar = 0.2 mm.

Figure 4. Epigenetic expression memory of endogenous loci repressed by SET-25. (A). DNA transposon expression in *set-25* mutants and at high temperature. Odds ratio quantifies the overlap (red loci, 'both') between log2 fold-change (FC) > 0. (B) FC expression three generations after a reduction in temperature from 25 to 20 °C. Kolmogorov–Smirnov (KS) test statistic and p-value shown. See Figures S11-S14 and Table S4 for other repeats, protein coding genes and analysis methods. (C) Expression of two DNA transposons at 25°C (F0) and for six generations after decreasing the temperature to 20°C determined by quantitative PCR (Table S3). *cdc-42* is a housekeeping gene as control. Expression is relative to animals grown at 20 °C in parallel. (D) Expression of the same DNA transposons is increased in *set-25* mutants.

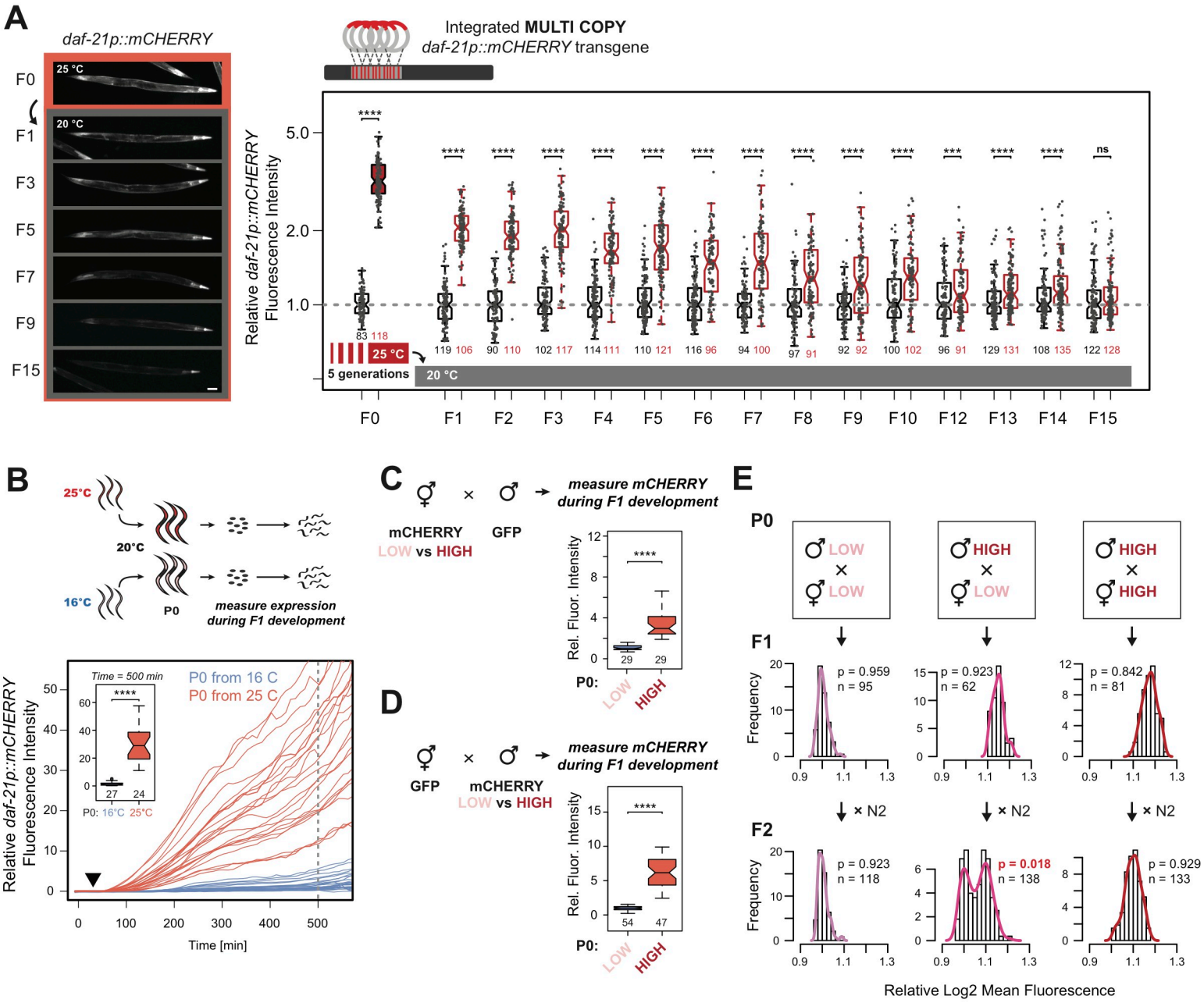
A
daf-21p::mCHERRY
F0
F1
F3
F5
F7
F9
F15
25 °C
20 °C
Integrated MULTI COPY
daf-21p::mCHERRY transgene
Relative daf-21p::mCHERRY Fluorescence Intensity
5.0
2.0
1.0
****
***
ns
83 118
119 106
90 110
102 117
114 111
110 121
116 96
94 100
97 91
92 92
100 102
96 91
129 131
108 135
122 128
25 °C
5 generations
20 °C
F0
F1
F2
F3
F4
F5
F6
F7
F8
F9
F10
F12
F13
F14
F15
B
25°C
20°C
16°C
P0
measure expression
during F1 development
Relative daf-21p::mCHERRY Fluorescence Intensity
Time = 500 min
P0 from 16 C
P0 from 25 C
P0: 16°C 25°C
27 24
Time [min]
C
mCHERRY
LOW vs HIGH
GFP
measure mCHERRY
during F1 development
Rel. Fluor. Intensity
29 29
P0:
LOW
HIGH
D
GFP
mCHERRY
LOW vs HIGH
measure mCHERRY
during F1 development
Rel. Fluor. Intensity
54 47
P0:
LOW
HIGH
E
P0
LOW × LOW
HIGH × LOW
HIGH × HIGH
F1
Frequency
p = 0.959
n = 95
p = 0.923
n = 62
p = 0.842
n = 81
× N2
F2
p = 0.923
n = 118
p = 0.018
n = 138
p = 0.929
n = 133
Relative Log2 Mean Fluorescence

Figure 1

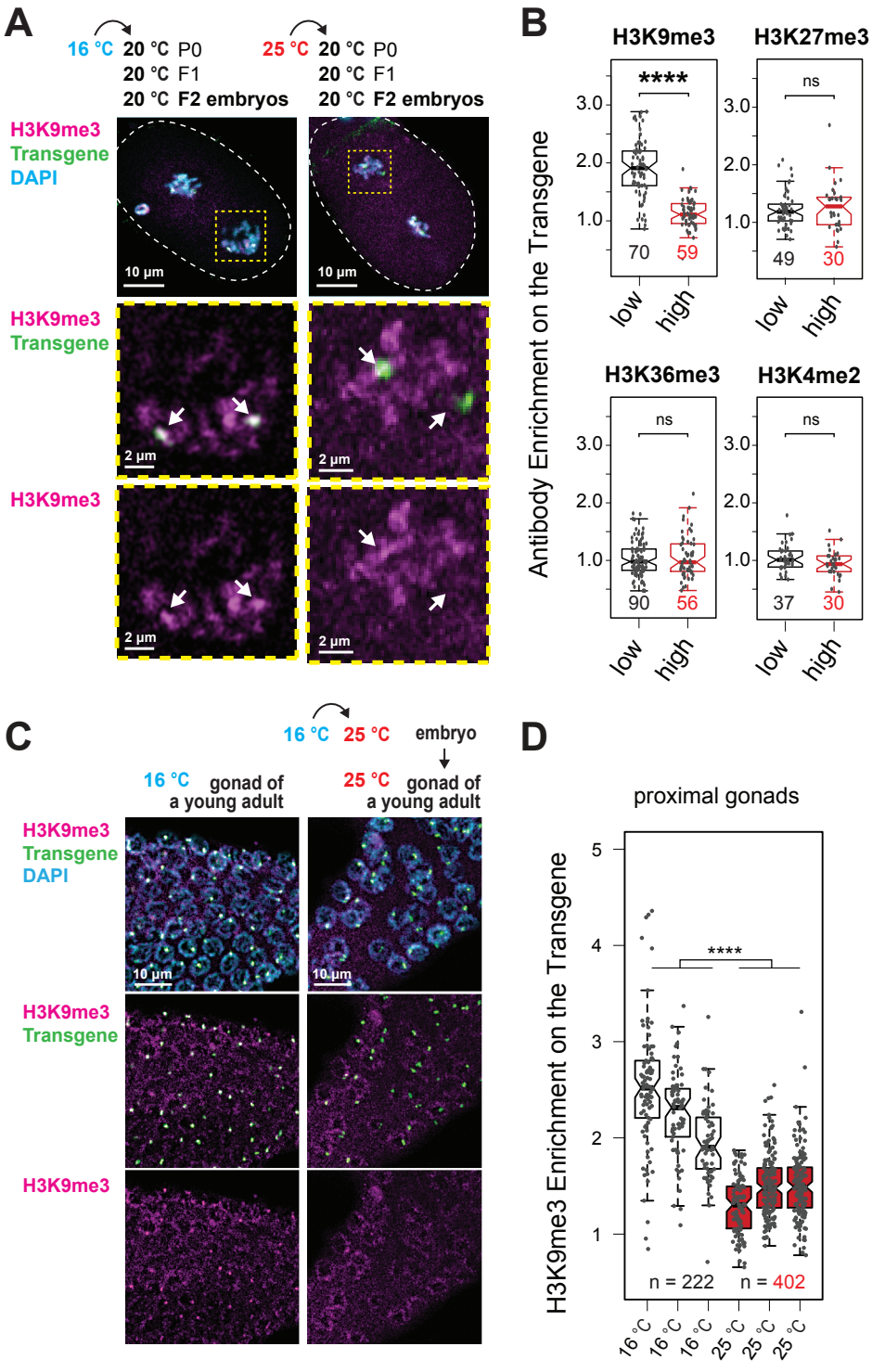
A
16 °C 20 °C P0
20 °C F1
20 °C F2 embryos
25 °C 20 °C P0
20 °C F1
20 °C F2 embryos
H3K9me3
Transgene
DAPI
H3K9me3
Transgene
H3K9me3
10 µm
2 µm
B
H3K9me3
H3K27me3
H3K36me3
H3K4me2
Antibody Enrichment on the Transgene
****
ns
70
59
49
30
90
56
37
30
low
high
C
16 °C 25 °C embryo
16 °C gonad of a young adult
25 °C gonad of a young adult
H3K9me3
Transgene
DAPI
H3K9me3
Transgene
H3K9me3
10 µm
D
proximal gonads
H3K9me3 Enrichment on the Transgene
****
n = 222
n = 402
16 °C
25 °C

Figure 2

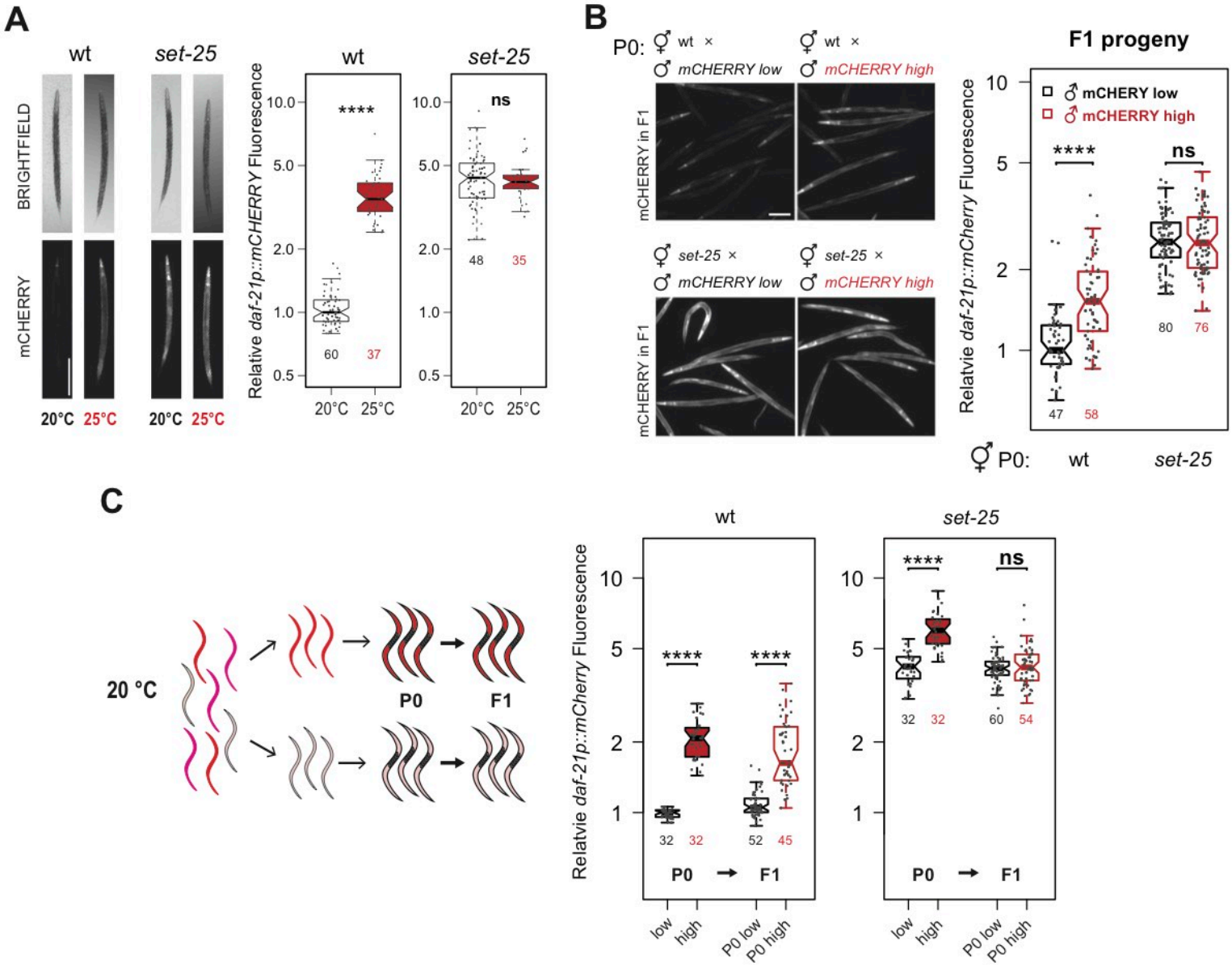
A
wt
set-25
BRIGHTFIELD
mCHERRY
20°C 25°C
20°C 25°C
wt
set-25
Relative daf-21p::mCHERRY Fluorescence
****
ns
60 37
48 35
20°C 25°C
20°C 25°C
B
P0: ♀ wt × ♂ mCHERRY low
♀ wt × ♂ mCHERRY high
♀ set-25 × ♂ mCHERRY low
♀ set-25 × ♂ mCHERRY high
mCHERRY in F1
mCHERRY in F1
F1 progeny
♂ mCHERY low
♂ mCHERRY high
Relatvie daf-21p::mCherry Fluorescence
****
ns
47 58
80 76
♀ P0: wt set-25
C
20 °C
P0
F1
wt
set-25
Relatvie daf-21p::mCherry Fluorescence
****
****
****
ns
32 32
52 45
32 32
60 54
P0 → F1
P0 → F1
low
high
P0 low
P0 high
low
high
P0 low
P0 high

Figure 3

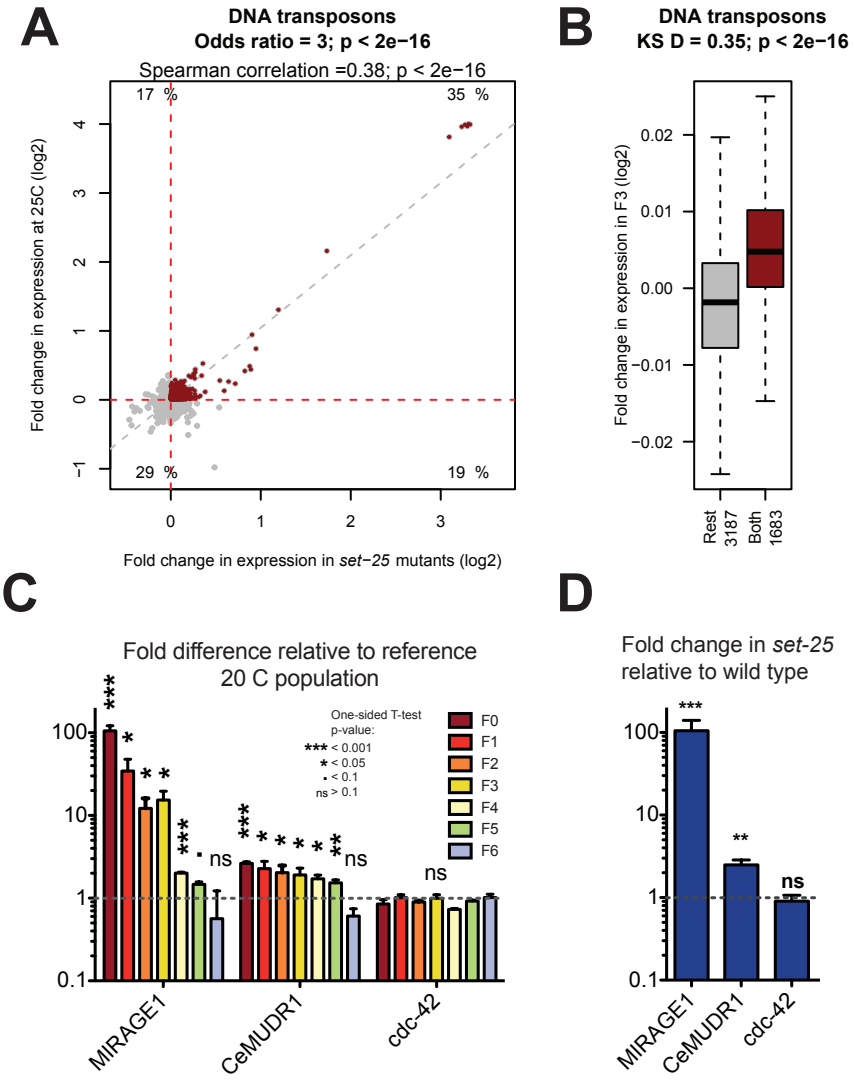
A
DNA transposons
Odds ratio = 3; p < 2e−16
Spearman correlation =0.38; p < 2e−16
17 %
35 %
29 %
19 %
Fold change in expression at 25C (log2)
Fold change in expression in set−25 mutants (log2)
B
DNA transposons
KS D = 0.35; p < 2e−16
Fold change in expression in F3 (log2)
Rest
3187
Both
1683
C
Fold difference relative to reference
20 C population
One-sided T-test
p-value:
*** < 0.001
* < 0.05
. < 0.1
ns > 0.1
F0
F1
F2
F3
F4
F5
F6
MIRAGE1
CeMUDR1
cdc-42
D
Fold change in set-25
relative to wild type
MIRAGE1
CeMUDR1
cdc-42

Figure 4

Supplementary Material

Contents

Materials and methods

Worm strains and culture conditions

All strains used in this study are listed in Table S2. Bristol N2 strain was used as the wild-type and all other strains used are derived from it. Worms were cultured using standard conditions (*27*) using NGM plates seeded with *Escherichia coli* OP-50 strain and grown at 20 °C unless stated otherwise in the text. In the multi-generational experiments worms were propagated by washing the gravid worms gently off the plate on day 1 of adulthood and extracting their embryos using an alkaline hypochlorite solution (bleaching) (*27*). Embryos were washed twice with M9 and plated on a fresh, OP-50 seeded NGM plate at an estimated concentration of 1000 embryos per plate.

Strain construction

The BCN1049 (*daf-21p::GFP*) and BCN1050 (*daf-21p::mCHERRY*) strains are described in (*28*). The single copy *daf-21p::GFP* reporter was generated by Knudra Transgenics.

Worm sorting

To make the 'high' and 'low' sorted cohorts a large population of about 2000 synchronized L4 worms was grown on a single OP50-seeded 90mm NGM plate. Between 32 and 40 single L4 worms were picked based on their extremely high or low fluorescence intensity relative to the population average. The adult worms were removed and imaged the following day having laid their embryos that constituted the next generation.

Temperature shifts

For the temperature shift, embryos were extracted from gravid adults as described above, plated on seeded NGM plates and put inside a 25 °C incubator. Shifting the worms back from 25 to 20 °C was always done at L4/young adult stage and measurements were taken on the following day when the worms reached adulthood. As a reference, a synchronized, age-matched population grown continuously at 20 °C was used.

Imaging of adult worms

Hermaphrodite worms in their first day of adulthood were picked from a plate and dropped into a single well of a 96-well plate (Nunc, optical bottom) filled with 90 µl of PBS, typically about 25 worms per well. 10 µl of 500mM sodium azide was then added to the well, which anesthetized the worms making them immobile. Worms were then manually separated from each other using an eyelash glued to a glass pipette and imaged within 30 minutes using a Leica DMI6000 B microscope equipped with 5x objective and Hamamatsu Orca Flash 4.0 digital camera and Lumen 200 metal arc lamp (Prior Scientific).

Measurement of fluorescent intensity of adult worms

Images were analyzed with Fiji/ImageJ software. Flat-field correction was done on both green and red channels by dividing by a background image of a well with no worms. The green channel captures the auto-fluorescence of worms and was used to identify the worms in images and create masks. The masks were then used to quantify mCHERRY intensity of fluorescence in each worm. For measurement of GFP intensity, DAPI channel was used to create masks from autofluorescence. Touching or overlapping worms as well as worms on edge of the image were discarded from analysis. Mean fluorescence intensity (Total Intensity/Area) was used as a measure of worm's brightness.

Time-lapse microscopy

To obtain embryos for time-lapse microscopy, 50 young gravid adult worms were selected and picked into 50 µl drop of PBS in a single well of a 3-well concavity slide. Worms were washed twice with 100 µl of PBS, then dissected with surgical needles releasing the embryos. 10 µl of 1:10 bleach solution (from 10 – 15 % stock) was added and after 20 seconds 50 µl of 5 % BSA in PBS was added which quenched the bleach solution. 4-cell stage embryos were selected based on morphology under a stereomicroscope and mouth-pipetted sequentially into the two

neighboring wells, each containing 100 µl of PBS. Using a mouth-pipette, washed embryos were transferred into a single well of a 96-well plate (Nunc, optical bottom) filled with 100 µl of PBS. To facilitate the imaging embryos were positioned near each other using a nose-hair pick. The procedure was done in parallel for 2 biological samples, each processed on a separate slide. The selection of 4-cell stage embryos was restrained to less than 10 minutes to ensure synchrony of embryos. Samples were imaged with a Leica DMI6000 B microscope equipped with Hamamatsu Orca Flash 4.0 digital camera and a motorized stage using a 10x objective. Images were acquired in Bright Field, GREEN and dsRED channel with a frequency of 1 image every 10 minutes. Data was analyzed in Fiji/ImageJ as described in (*28*)

Statistical analysis of fluorescence data

In the multi-generation analyses of expression level presented in Figures 1 and S1 we used a control (non-perturbed but otherwise identically treated) population of animals grown in parallel. At each time-point we tested for a difference between the expression in the experimental population and this control population. The experiments were performed using large cultures of worms (approximately 2000 animals per generation) with the two compared populations always grown and treated in parallel in identical conditions to control for any fluctuations arising from, for example, variation in the temperature of the incubators or the laboratory, or from variation in the light source during imaging. The populations were kept synchronised by bleaching. All analyses were performed in R (version 3.2.0). Default R parameters were used for generating boxplots: thick horizontal line represents the median, the boxed area spans the Interquartile Range (IQR) which encompasses 50% of data points, notches indicate the 95 % Confidence Interval of the Median, upper/lower whiskers extend to maximum/minimum value or 75 Percentile + 1.5*IQR/25 Percentile - 1.5*IQR whichever is less extreme. Two-sided Wilcoxon rank test was used for comparison of fluorescence intensities between different populations and the false discovery rate (FDR) was controlled using the Benjamini-Hochberg procedure. Student's T-test was used to analyze the quantitative RT-PCR data. For assessing data bimodality we used Hartigan's dip test.

Immunofluorescence

Embryos from bleached worms were freeze-cracked on liquid nitrogen, fixed with MeOH for 5 min followed by PFA 1% for 2min. After three washes in PBS 0.25% Triton X-100 (PBS-T) slides were blocked in PBS-T 0.5% BSA before overnight incubation with primary

antibody (H3K9me3 [#07-442, Millipore], H3K4me2 [#07-030, Millipore]. H3K27me3 [#07-449, Millipore], H3k36me3 [ab9050, Abcam]) at 4°C. After three washes with PBS-T, slides were incubated for 2 hours with secondary antibody (Alexa-555 anti-rabbit; Invitrogen) at room temperature. After three washes in PBS-T, samples were either mounted in Fluoroshield with DAPI mounting medium (Sigma) or processed for DNA-FISH. Images were taken using a Leica SP5 confocal microscope.

DNA-FISH and immunofluorescence

For combined histone antibody and DNA-FISH we first carried out antibody staining as described above. DNA-FISH was performed as in (*29*). Briefly, slides were fixed in formaldehyde fixative (3.7% formaldehyde, 80mM HEPES buffer (pH6.9), 1.6 mM MgSO4, 0.8 mM EGTA) for 15 min, rinsed in distilled water for 5min and immersed in 3:1 methanol:glacial acetic acid for 15 min. Samples were allowed to air dry. Probes for mCHERRY DNA were produced using the DIG-Nick Translation mix (Roche) and following the manufacturer's instructions. We applied the hybridization solution, consisting of labeled probe in 50% formamide, 2x saline sodium citrate (SSC) and 10% dextran sulfate, on each slide and denatured the samples at 80 °C for 10min. After an overnight hybridization at 37 °C, slides were washed in 50% formamide, 2x SSC at 37 °C for 15min, in 2xSSC at 37 °C for 7min and in PBS-T at room temperature for 5min. Samples were incubated with fluorescein-labeled antibody to digoxigenin (Roche) in PBS-T for 2h at 37 °C. After three washes in PBS-T samples were mounted in Fluoroshield with DAPI mounting medium (Sigma).

Single molecule FISH

Custom Stellaris® FISH Probes were designed against the GFP and endogenous *daf-21* mRNA by utilizing the Stellaris® FISH Probe Designer (Biosearch Technologies, Inc., Petaluma, CA) available online at www.biosearchtech.com/stellarisdesigner. Worms were hybridized with the GFP Stellaris FISH Probe set labeled with Quasar® dye and the *daf-21* set labeled with CAL Fluor® Red 590 simultaneously, following the manufacturer's instructions available online at www.biosearchtech.com/stellarisprotocols. Formamide concentration in hybridization and wash buffer was 15% and the total concentration of pooled probes was 25 nM. Hybridization was performed overnight at 30 C. Worms were imaged either using a 20x air objective or with an oil immersion 100x objective on a Leica DMI6000 B inverted microscope equipped with Hamamatsu Orca Flash 4.0 digital camera and a Lumen 200 metal arc lamp (Prior Scientific).

RNA sequencing

To prepare samples for sequencing, N2 worms grown continuously (>20 generations) at 20°C were shifted to 25 °C as L4 larvae and grown at that temperature for five generations. At the fifth generation, synchronized gravid adult worms were collected and RNA extracted. To obtain synchronized gravid F0 animals we bleached the previous generation to obtain the eggs, plated 1500 eggs per plate and grew the animals for 54 - 56 hours at 25 °C. These constituted the F0 ancestral population. Before reaching adulthood, at the L4 stage, a fraction of these animals were transferred to 20°C and propagated for three more generations at that temperature. To obtain synchronized gravid F3 animals, we bleached the previous generation to obtain the eggs, plated 1500 eggs per plate and grew the animals for 72 - 76 hours at 20°C. A control population was processed in parallel, starting from L4 animals grown continuously at 20°C. We used three plates for each replicate and three replicates for each condition. We monitored the cultures to ensure that they did no starve at any point. Animals were collected in M9 and RNA extracted using the TRIzol® extraction protocol (*30*).

Libraries for RNA-seq were prepared from 400 ng total RNA using the TruSeq Stranded Total RNA Library Prep Kit (ref. RS-122-2201, Illumina) using the included RiboZero reagents to deplete ribosomal RNAs according to manufacturer's instructions. The poly(A)-mRNA selection step was not carried out. Samples were sequenced with 2x50 bp paired-end reads using Illumina HiSeq v4 sequencing chemistry. All RNA-seq datasets are deposited in the NCBI GEO under accession GSE83528.

Copy number and transposon mobility estimation using quantitative real-time PCR

To measure relative copy number of the transgene and the transposons as well as transposon mobility we extracted DNA using a tissue extraction kit (QIAGEN), digested the remaining RNA with RNAse A and proceed to quantitative real-PCR using SYBR Green (Thermo Fischer Scientific). Analysis of the data was done using one point calibration method (*31*) and using a primer pair targeting csq-1 gene as reference. Primers used are listed in Table S3.

RNA expression measurement using quantitative real-time PCR

To measure relative expression levels of the transposons, RNA was isolated using the TRIzol® extraction protocol (*30*), digested with DNase I (Thermo Fisher Scientific) at 37 °C for 30

minutes, after which the enzyme was inactivated following the manufacturer's instructions. cDNA was produced using 250 ng of template RNA with SuperScript III Reverse transcriptase (Life Technologies) and Oligo dT primers. The remaining RNA was digested using RNaseH. cDNA was amplified using SYBR Green (Thermo Fischer Scientific), reference cDNA was used in each reaction plate for absolute quantitation and hence comparison between all samples. All expression was normalized to *cec-1* primer product. Primers used are listed in Table S3.

Computational analyses

Reads were mapped using tophat v2.1.0 (*32*) with the options --no-coverage-search -i 10 -I 40000 -g 20 to include multi-mapping at all the possible hits against the *C. elegans* genome (assembly WS215) from WormBase. Read counting at different genomic features was performed using featureCounts v1.5.1 (*33*) with the option -s 2 -B -p and the -M --fraction option. Multi mapping reads contribute as fractional counts towards the loci they map to (a read mapped X times adds 1/X to each locus). Each copy of a repeat was annotated separately. Re-analysis of the data using uniquely mapping reads showed very similar results. Collapsing repeats by subfamily led to the same conclusions. We used the *C. elegans* genome annotation from Ensembl release 70 and the RepeatMakser (http://www.repeatmasker.org) annotation from the UCSC genome browser. Pseudogenes overlapping repeats and repeats overlapping exons were removed. We only considered genes and repeats with a median of one or more reads (present in at least half the samples). Data scaling, normalization and tests for differential expression were performed with DESeq2 version 1.8.1 (*34*). DESeq2 applies a shrinkage, or regularization method, on log2 fold changes and these are the values plotted in the figures.

In addition, we processed the data (using the same filtering of genes with low read counts) using the standard limma pipeline to estimate the true biological correlation using the genas function (*35*). For the transformation of reads to logCPM counts we used a prior of 1 and for the calculation of differential expression we used limma-trend. The linear model was then passed to the genas function to estimate the biological correlation between the contrast of *set-25* mutants against the wt controls at 20°C and the 25°C wt animals against the 20°C wt animals. Results from a number of different sub-setting methods of the genas function are shown in Table S4. This analysis confirmed that DNA transposons and other repeats had a strong positive correlation between the two different contrasts.

Figure S1. Expression from heterochromatic repetitive arrays but not from a single copy transgenes transmits long-lasting environmental information between generations.

(A) A single copy *daf-21p::GFP* transgene has higher somatic expression at 25 °C but this difference is only maintained in the immediate progeny after transferring to 20 °C. (B) 9 generation memory of high expression from a *daf-21p::GFP* multicopy transgene when transferring animals to 20 °C after five generations at 25 °C. (C) Growing animals at 25 °C for 48 hours from embryos to the L4 stage is sufficient to mount a heritable change in transgene expression that declines gradually over 7 generations. In all experiments stage-matched worms kept constantly at 20 °C were used as a reference for normalization (black bars). Expression was quantified in adults. False discovery rates (FDR) were controlled using the Benjamini-Hochberg procedure. q-values: **** $q < 0.0001$, *** $q<0.001$, ** $q<0.001$, ns $q > 0.05$ (Wilcoxon rank test). Y-axes in log scale. Sample size indicated below each boxplot. (D) No increase in *daf-21p::GFP* multicopy transgene copy number at high temperature detected by quantitative real-time PCR. Strain cultivated at 20 or at 25 °C for 5-6 generations. Copy number is normalized to the *csq-1* genomic region. See Table S3 for primers.

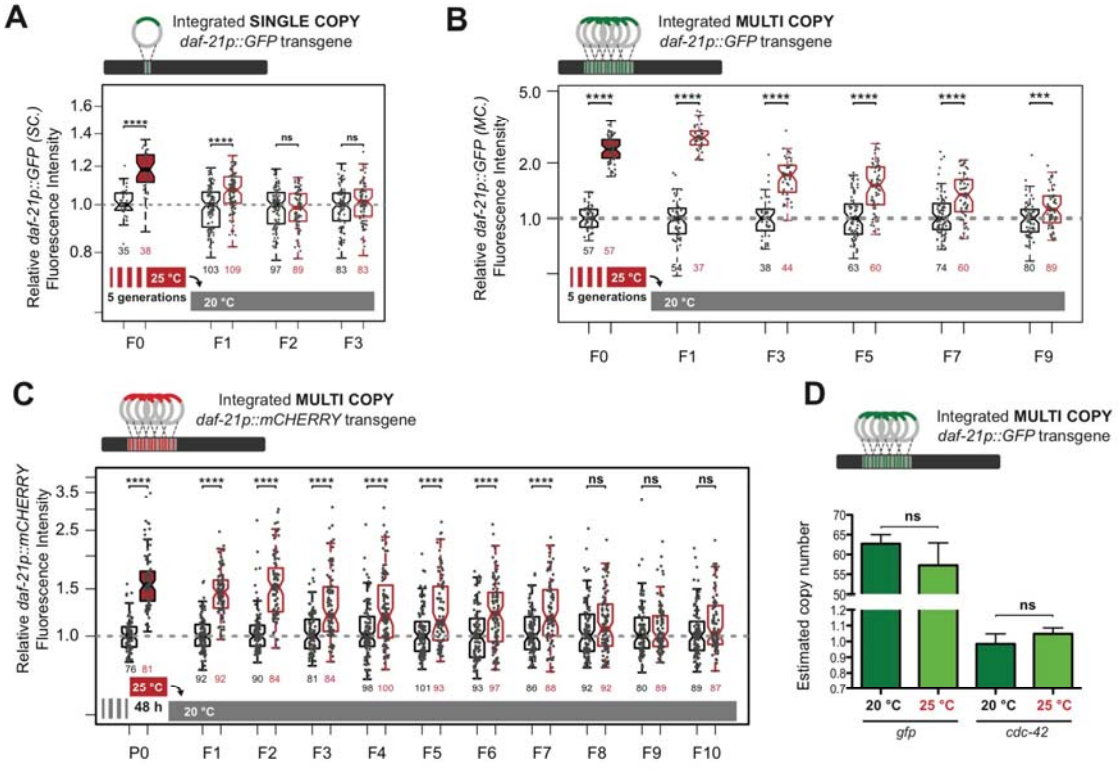
A
Integrated SINGLE COPY
daf-21p::GFP transgene
Relative daf-21p::GFP (SC.)
Fluorescence Intensity
25 °C
5 generations
20 °C
F0
F1
F2
F3
B
Integrated MULTI COPY
daf-21p::GFP transgene
Relative daf-21p::GFP (MC.)
Fluorescence Intensity
25 °C
5 generations
20 °C
F0
F1
F3
F5
F7
F9
C
Integrated MULTI COPY
daf-21p::mCHERRY transgene
Relative daf-21p::mCHERRY
Fluorescence Intensity
25 °C
48 h
20 °C
P0
F1
F2
F3
F4
F5
F6
F7
F8
F9
F10
D
Integrated MULTI COPY
daf-21p::GFP transgene
Estimated copy number
20 °C
25 °C
20 °C
25 °C
gfp
cdc-42

Figure S2. The *daf-21p::GFP* multicopy reporter is activated during embryonic development.

Two color single molecule FISH (smFISH) was used to simultaneously detect endogenous *daf-21* mRNA transcripts and *gfp* mRNA transcribed from the integrated multicopy *daf-21p::GFP* transcriptional reporter. A representative embryo from each stage of development is shown. In red squares: magnification of the indicated region.

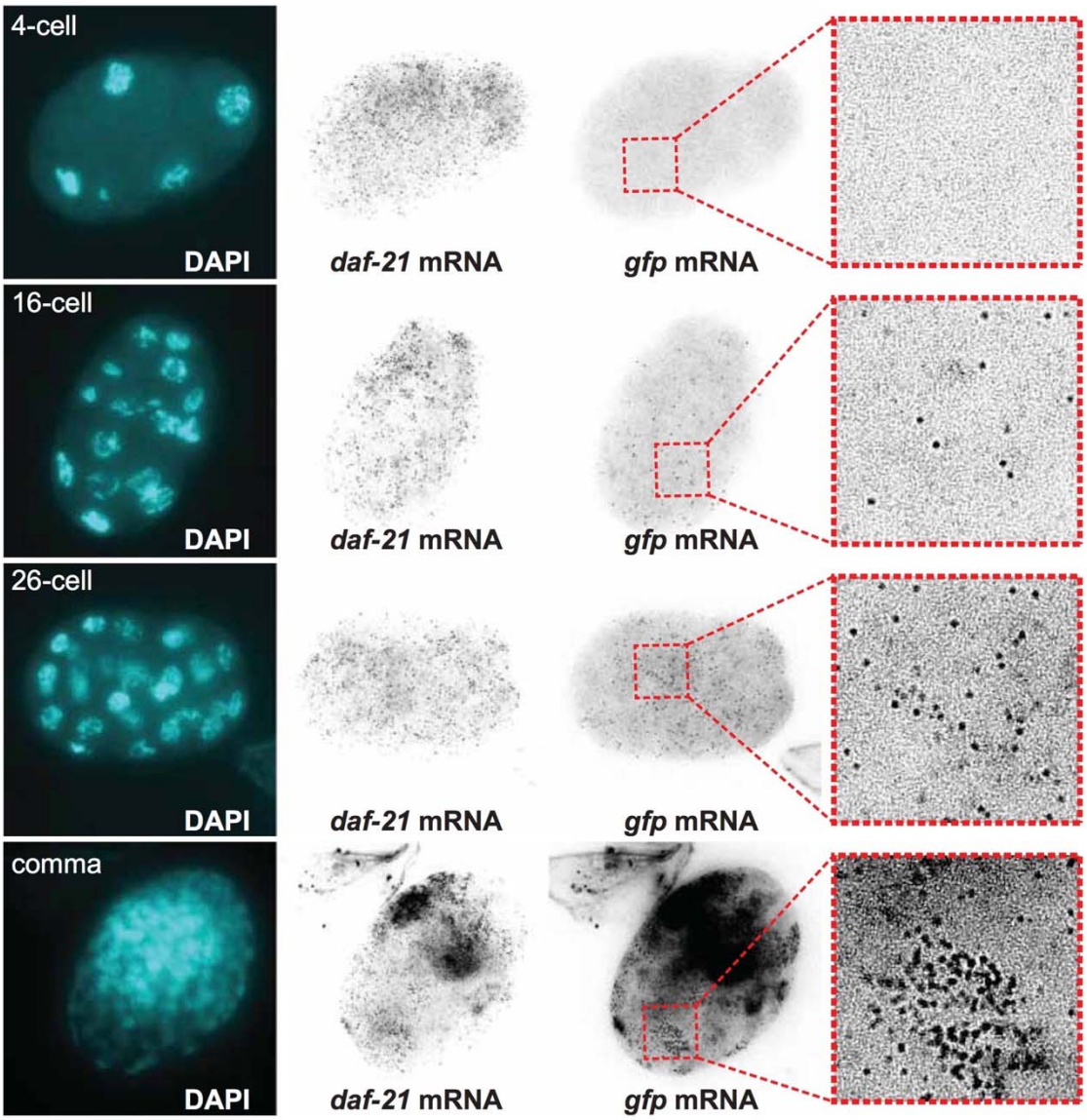
4-cell
DAPI
daf-21 mRNA
gfp mRNA
16-cell
DAPI
daf-21 mRNA
gfp mRNA
26-cell
DAPI
daf-21 mRNA
gfp mRNA
comma
DAPI
daf-21 mRNA
gfp mRNA

Figure S3. Inheritance of expression levels from sorted high and low expressing animals.

(A) L4 larvae from a population maintained at 20°C were manually sorted into *daf-21p::mCHERRY* 'high' and 'low' cohorts. The next day the F1 embryos were extracted and the transgene expression quantified during embryonic development (B). Quantification in (C) at the time-point indicated by the dotted line in (B).

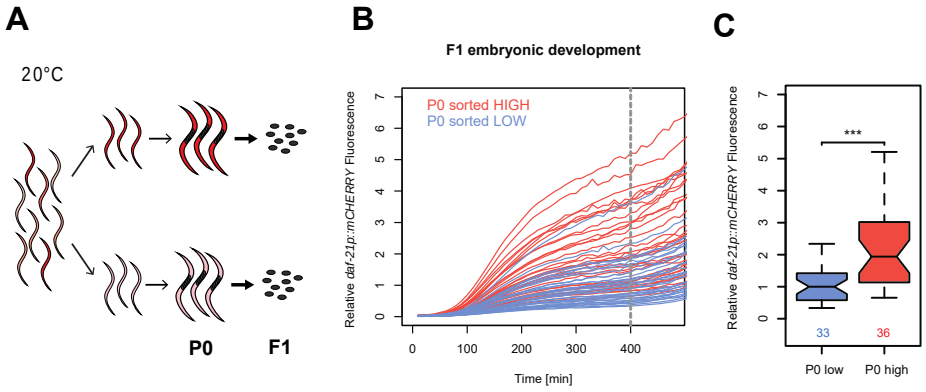
A
20°C
P0
F1
B
F1 embryonic development
P0 sorted HIGH
P0 sorted LOW
Relative daf-21p::mCHERRY Fluorescence
Time [min]
C
***
33
36
P0 low
P0 high

Figure S4. Distinguishing *cis* and *trans* inheritance (experimental design for Figure 1E).

Particulate inheritance in *cis* with the array predicts a bimodal expression distribution when animals expressing 'high' and 'low' levels of mCHERRY (high and low epi-alleles) are mated and subsequently crossed with wild-type animals whereas *trans* inheritance (e.g. cytoplasmic or small RNA-mediated inheritance) predicts a unimodal distribution.

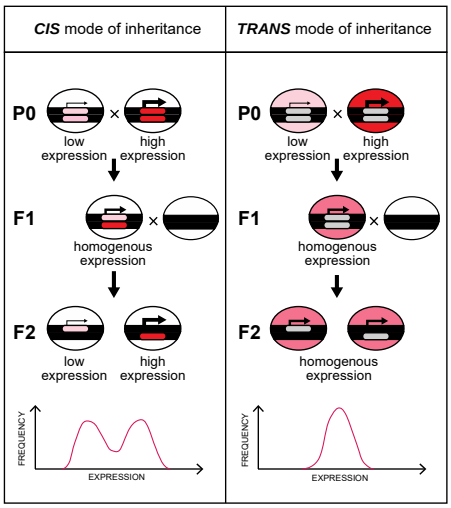
CIS mode of inheritance
TRANS mode of inheritance
P0
low expression
high expression
F1
homogenous expression
F2
low expression
high expression
homogenous expression
FREQUENCY
EXPRESSION

Figure S5. No changes in H3K4me2, H3K36me3 and H3K27me3 on the transgene array in animals expressing different level of *daf-21p::mCHERRY*.

(A) Examples of early stage embryos stained with DAPI (blue), DNA FISH probe complementary to mCHERRY (green) and anti-H3K4me2, anti-H3K27me3 or anti-H3K36me3 (pink). White arrows indicate the transgene locus identified through DNA FISH staining. Data quantified in Figure 2. (B) *set-25(n5021)* embryos show no detectable H3K9me3 while the H3K4me2 mark is unaffected.

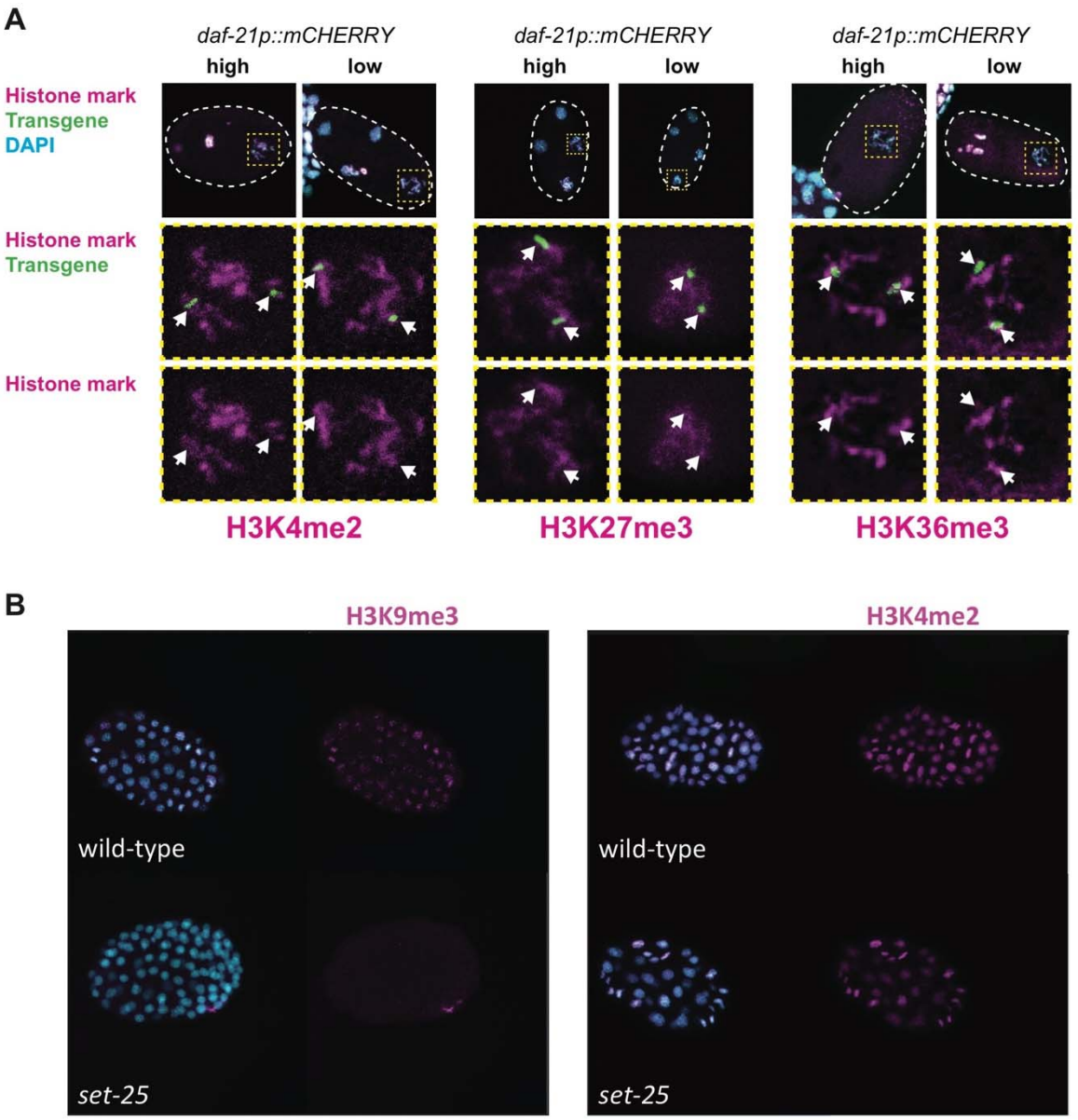
A
daf-21p::mCHERRY
high
low
Histone mark
Transgene
DAPI
Histone mark
Transgene
Histone mark
H3K4me2
H3K27me3
H3K36me3
B
H3K9me3
H3K4me2
wild-type
wild-type
set-25
set-25

Figure S6. Differences in H3K9me3 levels between 'high' and 'low' expressing animals are maintained in the late embryos

Left panels: examples of late embryos stained with DAPI (blue), DNA FISH probe complementary to mCHERRY (green) and anti-H3K9me3 (pink). White squares are enlarged to show more details. Scale bar is 50µm. Right panel: Quantification of H3K9me3 enrichment at the transgene array in late embryos (Wilcoxon rank test). The number of embryos quantified is shown for each condition.

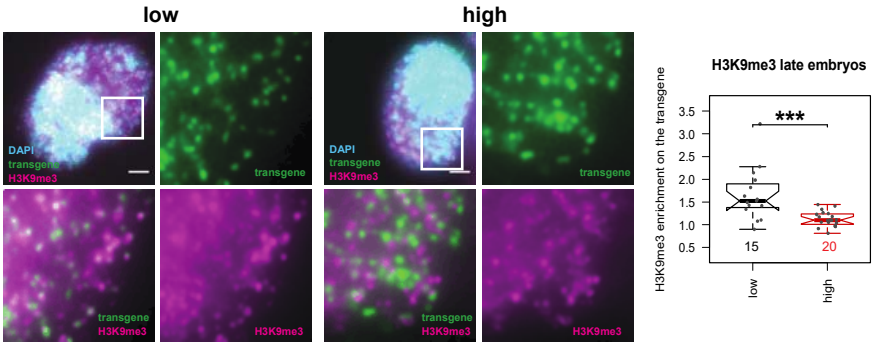
low
high
DAPI
transgene
H3K9me3
transgene
H3K9me3
H3K9me3 late embryos
H3K9me3 enrichment on the transgene
***
3.5
3.0
2.5
2.0
1.5
1.0
0.5
15
20
low
high

Figure S7. No germline expression of multi-copy transgene assayed by smFISH and fluorescence.

(A) Low and high *expressing daf-21p::GFP* (high-copy) L1 larvae mixed and stained with smFISH probes targeting *gfp* and endogenous *daf-21*. GFP protein fluorescence in whole larvae correlates with *gfp* mRNA detected with smFISH (Pearson correlation = 0.96). (B) High-copy *daf-21p::GFP* transgene is not expressed in the germline as exemplified by micrographs of L1 (B) and L4 (C) stage animals. Endogenous daf-21 transcript is readily detected in the germline, whereas the gfp is seen in somatic cells of the gonad (Z1, sheath cells). Animals grown for at least 5 generations at 25°C were used. (D) Dissected gonad of an animal carrying *daf-21p::mCHERRY* high-copy transgene. Expression is seen only in the somatic cells of the gonad such as sheath cells and spermatheca.

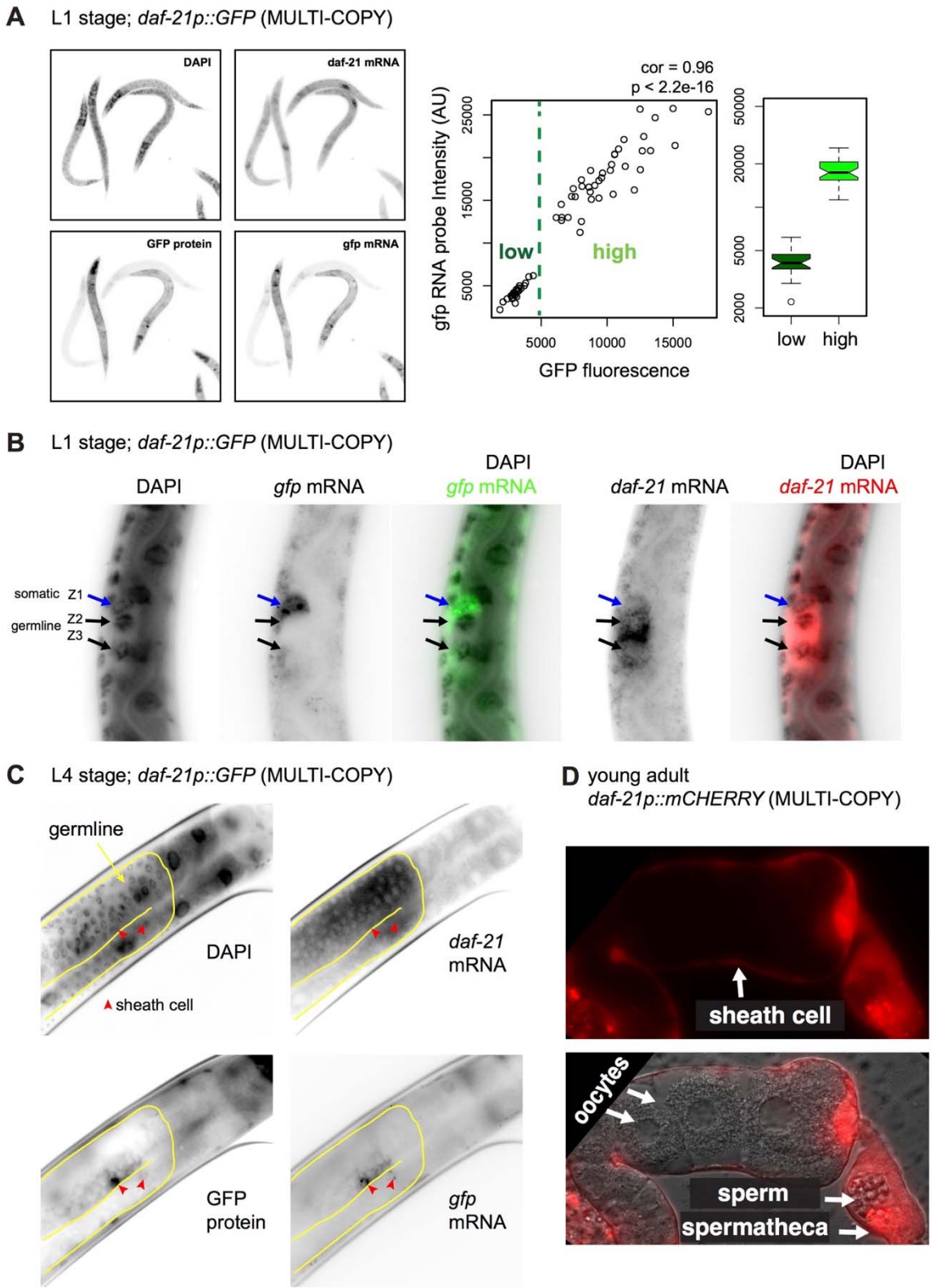
A
L1 stage; daf-21p::GFP (MULTI-COPY)
DAPI
daf-21 mRNA
GFP protein
gfp mRNA
cor = 0.96
p < 2.2e-16
gfp RNA probe Intensity (AU)
GFP fluorescence
low
high
B
L1 stage; daf-21p::GFP (MULTI-COPY)
DAPI
gfp mRNA
DAPI
gfp mRNA
daf-21 mRNA
DAPI
daf-21 mRNA
somatic Z1
germline Z2
Z3
C
L4 stage; daf-21p::GFP (MULTI-COPY)
germline
DAPI
sheath cell
daf-21
mRNA
GFP
protein
gfp
mRNA
D
young adult
daf-21p::mCHERRY (MULTI-COPY)
sheath cell
oocytes
sperm
spermatheca

Figure S8. Development at high temperature lowers H3K9me3 enrichment on the transgene array in distal germline nuclei.

Gonads were extracted from adult worms shifted from 16 to 25 °C during embryonic development, fixed, stained and compared to those from animals kept constantly at 16 °C. H3K9me3 is depleted from the transgene locus in the distal gonads when animals develop at elevated temperature. Each boxplot in quantifies the nuclei of a single gonad. P values: **** $p < 0.0001$, ns $p > 0.05$ (Wilcoxon rank test). Y-axes in log scale

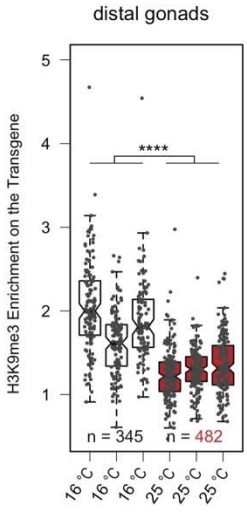
distal gonads
H3K9me3 Enrichment on the Transgene
5
4
3
2
1
****
n = 345
n = 482
16 °C
16 °C
16 °C
25 °C
25 °C
25 °C

Figure S9. Genetic tests for maternal requirement for epigenetic transmission

(A) MET-1, MET-2, HRDE-1, NRDE-2 and SPR-5 do not need to be maternally supplied to an embryo for the transmission of a temperature-induced change in *daf-21p::mCHERRY* expression. Experimental design as in Figure 3B. P-values: *** $p < 0.001$, ns $p > 0.05$ (Wilcoxon rank test). Y-axis in log scale. (B) MES-2 and MES-4 do not need to be maternally supplied to an embryo for the transmission of a temperature-induced change in *daf-21p::mCHERRY* expression. Phenotypically genotyped *mes-2* and *mes-4* homozygous progeny of *mes-2/+* and *mes-4/+* parents were used for the crosses. Phenotypic identification of the genotypes was possible because of linkage of the mutant *mes-2* and *mes-4* alleles to recessive alleles that cause Uncoordinated and Dumpy phenotypes, respectively. P values: *** $p < 0.001$ (Wilcoxon rank test). Y axis in log scale.

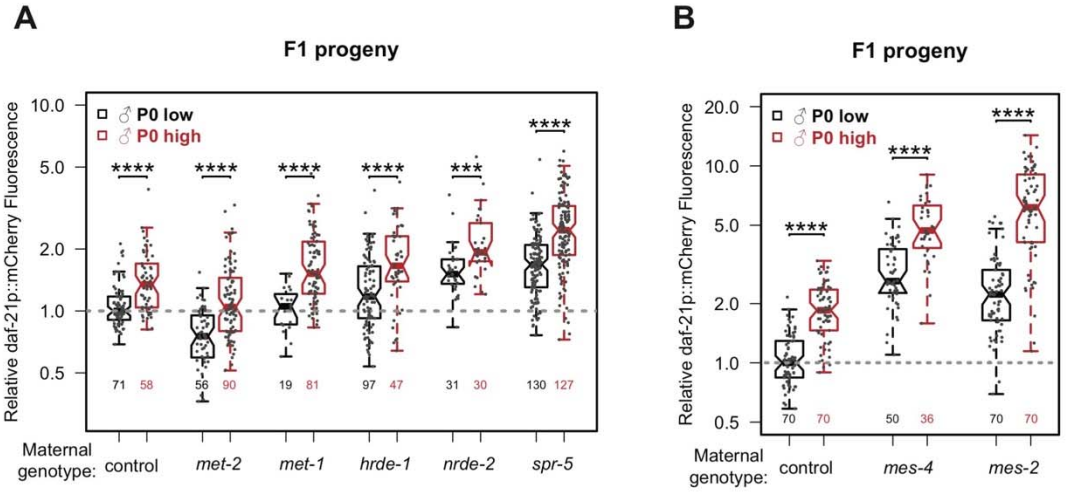
A
F1 progeny
♂ P0 low
♂ P0 high
Relative daf-21p::mCherry Fluorescence
10.0
5.0
2.0
1.0
0.5
****
****
****
****
***
****
71 58
56 90
19 81
97 47
31 30
130 127
Maternal genotype:
control
met-2
met-1
hrde-1
nrde-2
spr-5
B
F1 progeny
♂ P0 low
♂ P0 high
Relative daf-21p::mCherry Fluorescence
20.0
10.0
5.0
2.0
1.0
0.5
****
****
****
70 70
50 36
70 70
Maternal genotype:
control
mes-4
mes-2

Figure S10. Working model. High temperature reduces SET-25-mediated repression. After a return to low temperature it takes multiple generations for repression mediated by H3K9me3 (red flags) to be fully re-established on the multi-copy transgene array.

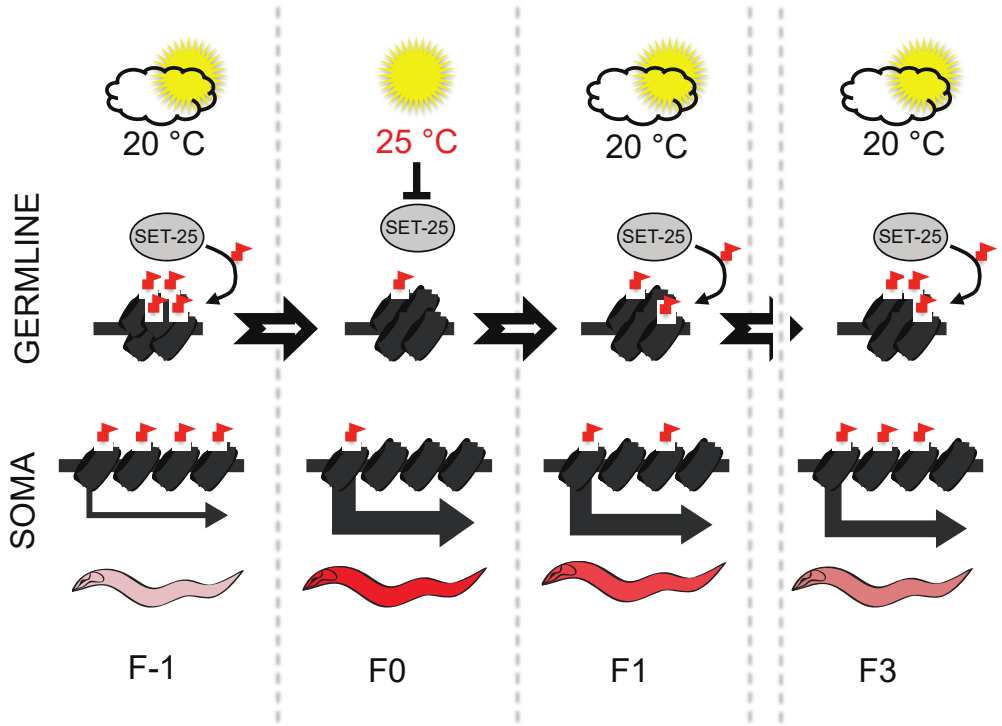
20 °C
25 °C
20 °C
20 °C
GERMLINE
SET-25
SET-25
SET-25
SET-25
SOMA
F-1
F0
F1
F3

Figure S11. Expression of repeat classes and protein-coding genes in *set-25* mutants, at high temperature (25 °C) and three generations after a change in temperature from 25 to 20 °C). Expression is quantified using multi-mapping reads as in Figure 4.

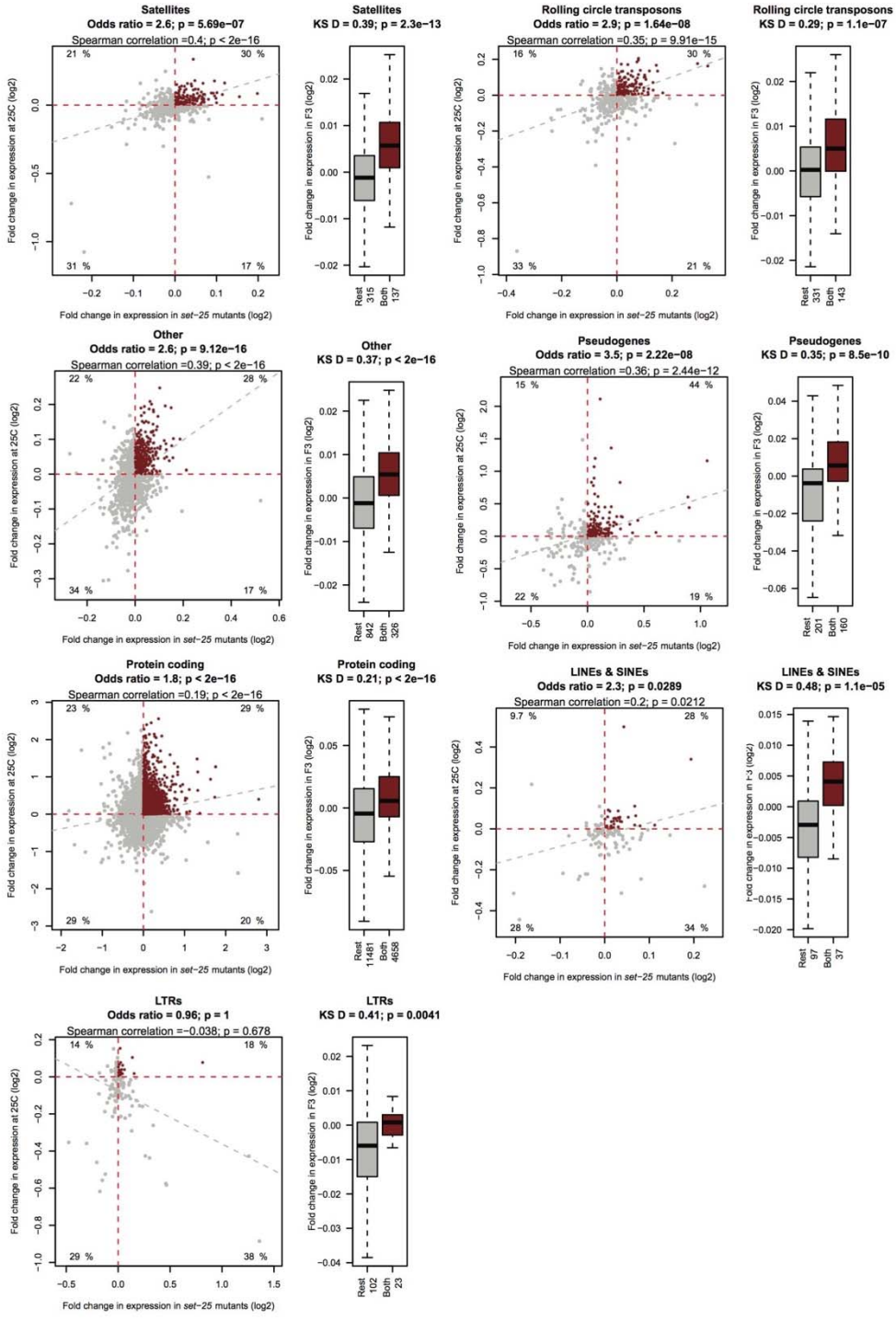
Satellites
Odds ratio = 2.6; p = 5.69e−07
Spearman correlation =0.4; p < 2e−16
21 %
30 %
31 %
17 %
Fold change in expression at 25C (log2)
Fold change in expression in set−25 mutants (log2)
Satellites
KS D = 0.39; p = 2.3e−13
Fold change in expression in F3 (log2)
Rest 315
Both 137
Rolling circle transposons
Odds ratio = 2.9; p = 1.64e−08
Spearman correlation =0.35; p = 9.91e−15
16 %
30 %
33 %
21 %
Rolling circle transposons
KS D = 0.29; p = 1.1e−07
Rest 331
Both 143
Other
Odds ratio = 2.6; p = 9.12e−16
Spearman correlation =0.39; p < 2e−16
22 %
28 %
34 %
17 %
Other
KS D = 0.37; p < 2e−16
Rest 842
Both 326
Pseudogenes
Odds ratio = 3.5; p = 2.22e−08
Spearman correlation =0.36; p = 2.44e−12
15 %
44 %
22 %
19 %
Pseudogenes
KS D = 0.35; p = 8.5e−10
Rest 201
Both 160
Protein coding
Odds ratio = 1.8; p < 2e−16
Spearman correlation =0.19; p < 2e−16
23 %
29 %
29 %
20 %
Protein coding
KS D = 0.21; p < 2e−16
Rest 11481
Both 4658
LINEs & SINEs
Odds ratio = 2.3; p = 0.0289
Spearman correlation =0.2; p = 0.0212
9.7 %
28 %
28 %
34 %
LINEs & SINEs
KS D = 0.48; p = 1.1e−05
Rest 97
Both 37
LTRs
Odds ratio = 0.96; p = 1
Spearman correlation =−0.038; p = 0.678
14 %
18 %
29 %
38 %
LTRs
KS D = 0.41; p = 0.0041
Rest 102
Both 23

Figure S12. Expression of repeat classes and pseudogenes in *set-25* mutants, at high temperature (25 °C) and three generations after a change in temperature from 25 to 20 °C) combining repeats by subfamily. Expression is quantified as in Figure 4 but combining all reads from repeats belonging to the same subfamily.

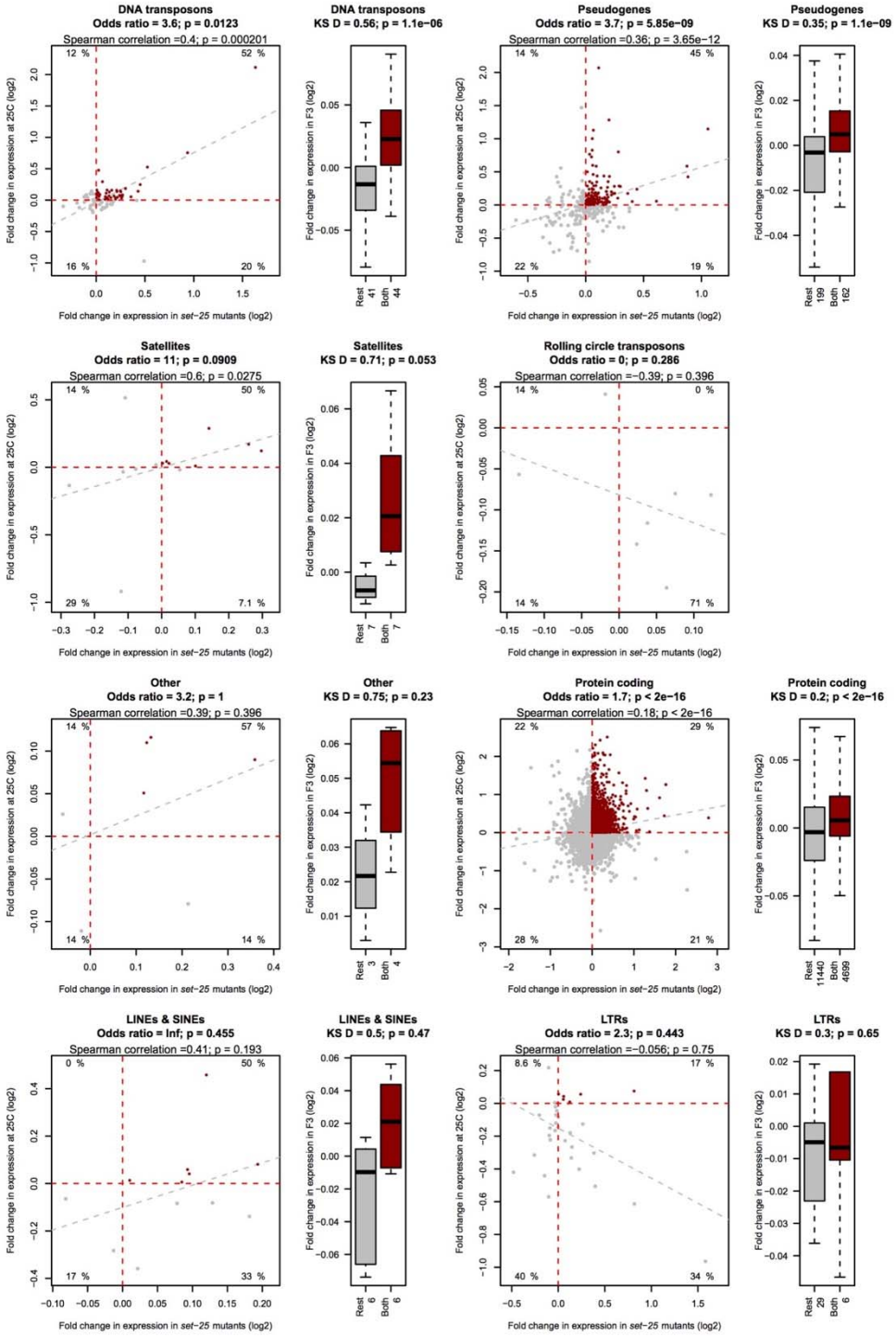
DNA transposons
Odds ratio = 3.6; p = 0.0123
Spearman correlation =0.4; p = 0.000201
DNA transposons
KS D = 0.56; p = 1.1e−06
Pseudogenes
Odds ratio = 3.7; p = 5.85e−09
Spearman correlation =0.36; p = 3.65e−12
Pseudogenes
KS D = 0.35; p = 1.1e−09
Satellites
Odds ratio = 11; p = 0.0909
Spearman correlation =0.6; p = 0.0275
Satellites
KS D = 0.71; p = 0.053
Rolling circle transposons
Odds ratio = 0; p = 0.286
Spearman correlation =−0.39; p = 0.396
Other
Odds ratio = 3.2; p = 1
Spearman correlation =0.39; p = 0.396
Other
KS D = 0.75; p = 0.23
Protein coding
Odds ratio = 1.7; p < 2e−16
Spearman correlation =0.18; p < 2e−16
Protein coding
KS D = 0.2; p < 2e−16
LINEs & SINEs
Odds ratio = Inf; p = 0.455
Spearman correlation =0.41; p = 0.193
LINEs & SINEs
KS D = 0.5; p = 0.47
LTRs
Odds ratio = 2.3; p = 0.443
Spearman correlation =−0.056; p = 0.75
LTRs
KS D = 0.3; p = 0.65
Fold change in expression at 25C (log2)
Fold change in expression in set−25 mutants (log2)
Fold change in expression in F3 (log2)
Rest
Both

Figure S13. Expression of repeat classes and pseudogenes in *set-25* mutants, at high temperature (25 °C) and three generations after a change in temperature from 25 to 20 °C) using uniquely mapping reads. Expression is quantified as in Figure 4 but only using uniquely mapping sequencing reads.

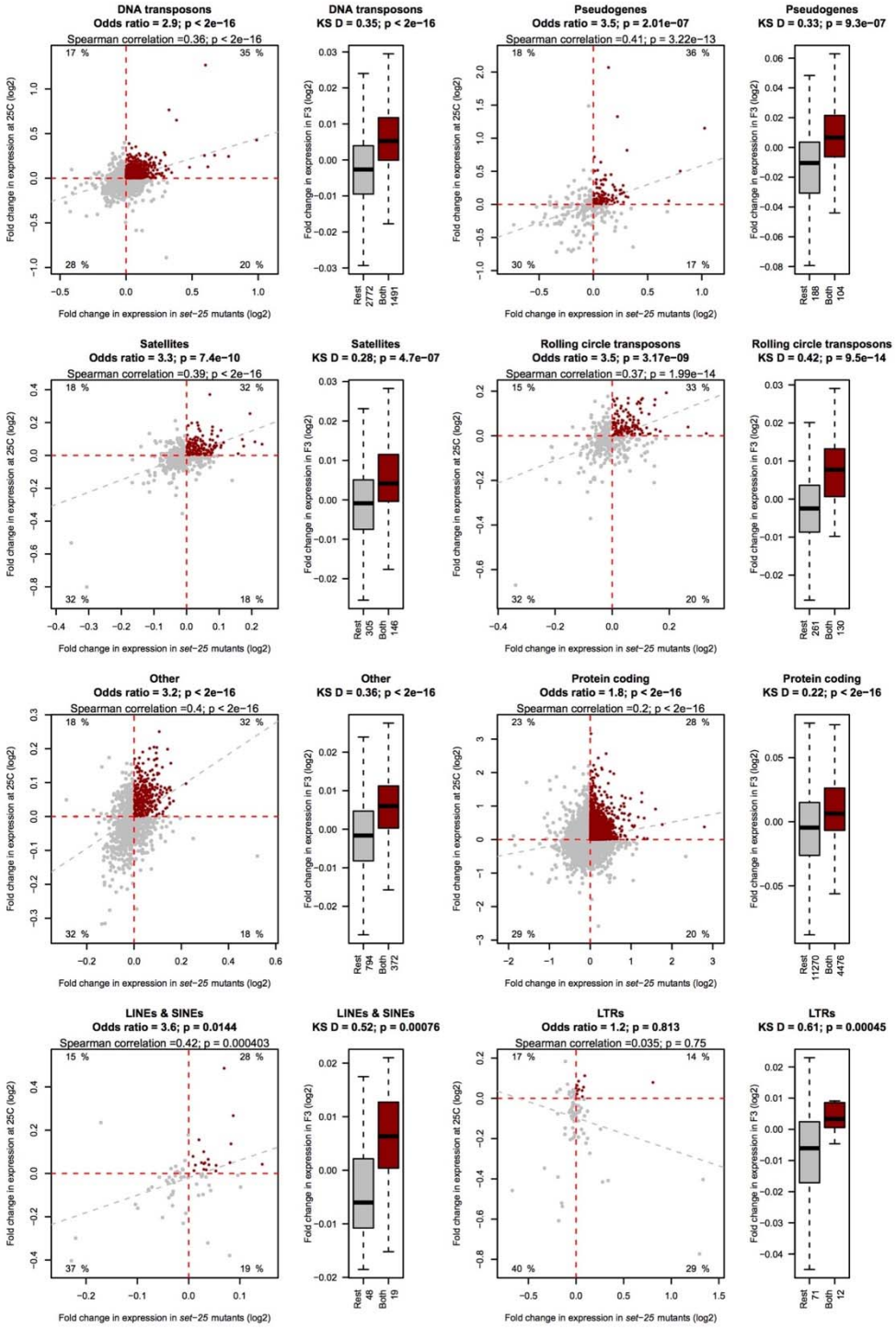
DNA transposons
Odds ratio = 2.9; p < 2e−16
Spearman correlation =0.36; p < 2e−16
17 %
35 %
28 %
20 %
Fold change in expression at 25C (log2)
Fold change in expression in set−25 mutants (log2)
DNA transposons
KS D = 0.35; p < 2e−16
Fold change in expression in F3 (log2)
Rest 2772
Both 1491
Pseudogenes
Odds ratio = 3.5; p = 2.01e−07
Spearman correlation =0.41; p = 3.22e−13
18 %
36 %
30 %
17 %
Pseudogenes
KS D = 0.33; p = 9.3e−07
Rest 188
Both 104
Satellites
Odds ratio = 3.3; p = 7.4e−10
Spearman correlation =0.39; p < 2e−16
18 %
32 %
32 %
18 %
Satellites
KS D = 0.28; p = 4.7e−07
Rest 305
Both 146
Rolling circle transposons
Odds ratio = 3.5; p = 3.17e−09
Spearman correlation =0.37; p = 1.99e−14
15 %
33 %
32 %
20 %
Rolling circle transposons
KS D = 0.42; p = 9.5e−14
Rest 261
Both 130
Other
Odds ratio = 3.2; p < 2e−16
Spearman correlation =0.4; p < 2e−16
18 %
32 %
32 %
18 %
Other
KS D = 0.36; p < 2e−16
Rest 794
Both 372
Protein coding
Odds ratio = 1.8; p < 2e−16
Spearman correlation =0.2; p < 2e−16
23 %
28 %
29 %
20 %
Protein coding
KS D = 0.22; p < 2e−16
Rest 11270
Both 4476
LINEs & SINEs
Odds ratio = 3.6; p = 0.0144
Spearman correlation =0.42; p = 0.000403
15 %
28 %
37 %
19 %
LINEs & SINEs
KS D = 0.52; p = 0.00076
Rest 48
Both 19
LTRs
Odds ratio = 1.2; p = 0.813
Spearman correlation =0.035; p = 0.75
17 %
14 %
40 %
29 %
LTRs
KS D = 0.61; p = 0.00045
Rest 71
Both 12

Figure S14. Changing the threshold for expression de-repression does not change the conclusion that loci de-repressed in *set-25* mutants and at 25 °C maintain elevated expression three generations after a reduction in temperature from 25 to 20 °C.

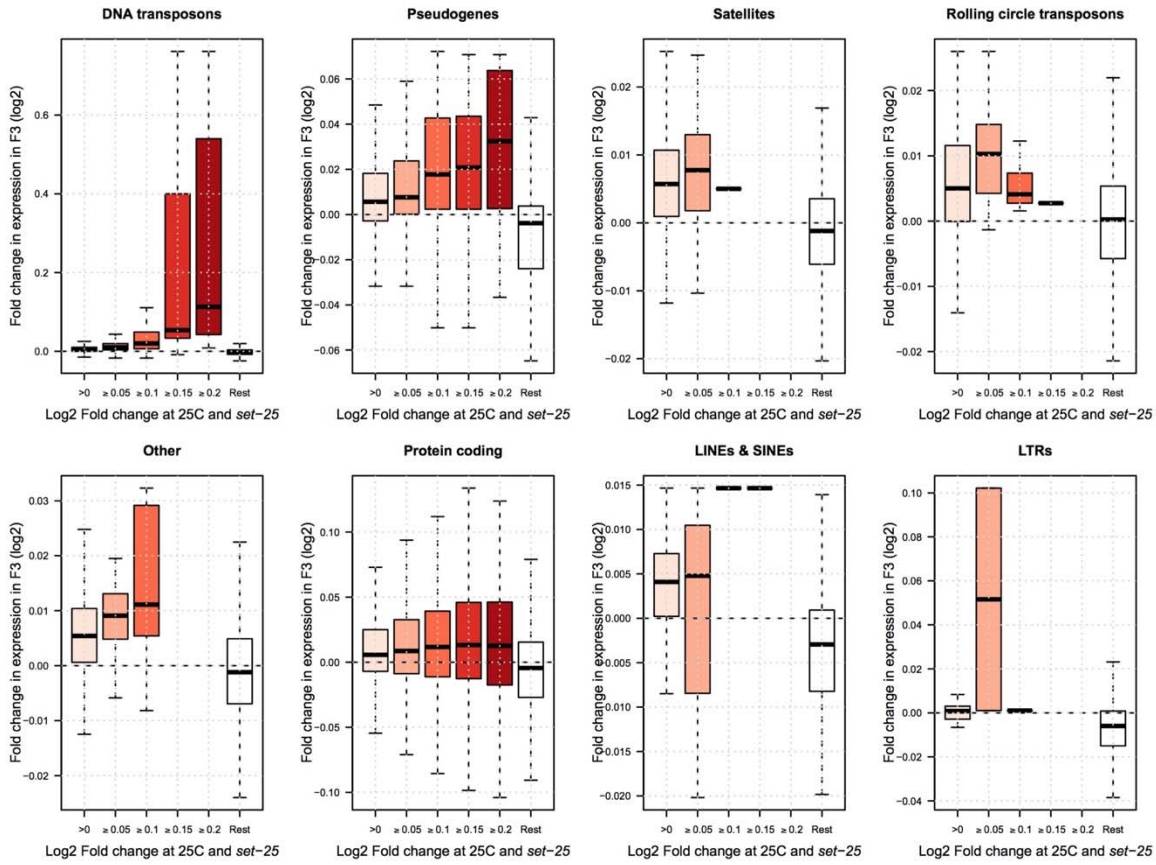
DNA transposons
Pseudogenes
Satellites
Rolling circle transposons
Other
Protein coding
LINEs & SINEs
LTRs
Fold change in expression in F3 (log2)
>0
≥ 0.05
≥ 0.1
≥ 0.15
≥ 0.2
Rest
Log2 Fold change at 25C and set−25

Figure S15. Measurement of transposon copy-number (A) and mobilization (B) using quantitative real-time PCR (RT-qPCR). Primer pairs amplified genomic loci of the elements assayed with RT-qPCR (Figure 4). Transposon mobility was assayed for several unique loci using an internal primer located within a transposon and an external one located outside of the transposon element. No significant differences were observed between worms grown at 20°C and 25°C. See Table S3 for primers.

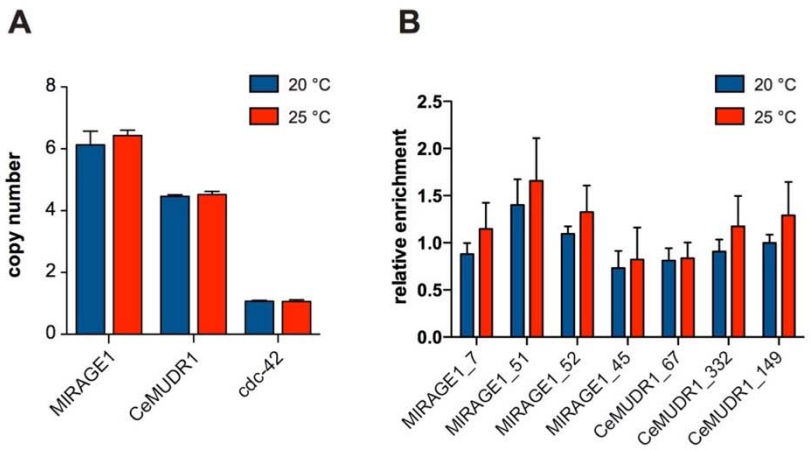
A
B
20 °C
25 °C
copy number
8
6
4
2
0
MIRAGE1
CeMUDR1
cdc-42
relative enrichment
2.5
2.0
1.5
1.0
0.5
0.0
MIRAGE1_7
MIRAGE1_51
MIRAGE1_52
MIRAGE1_45
CeMUDR1_67
CeMUDR1_332
CeMUDR1_149

Table S1. Additional multicopy transgenes exhibit trans-generational memory of high temperature-induced increases in expression.

				elevated expression after shift to 20 °C		
Strain	**Transgene**	**Copy Number**	**UP at 25 °C**	**F1**	**F2**	**F5**
BCN1050	*daf-21::mCHERRY*	MULTI	YES	YES	YES	YES
BCN1049	*daf-21::GFP*	MULTI	YES	YES	YES	YES
BCN1082	*daf-21::GFP*	SINGLE	YES	YES	NO	NO
CL2166	*gst-4::GFP*	MULTI	YES	YES	YES	YES
CF1553	*sod-3::GFP*	MULTI	YES	YES	YES	YES
TJ375	*hsp-16.2::GFP*	MULTI	YES*	YES*	nd	nd
SJ4005	*hsp-4::GFP*	MULTI	YES	NO	nd	nd
MH1870	*sur-5::GFP*	MULTI	YES	NO	NO	nd
KM267	*hsp-16.41::hlh-1 + pRF4 (rol-6)*	MULTI	YES**	YES**	YES**	YES**

nd = not determined

* expression induced by 30min heat shock at 34 °C

** expression inferred from frequency of 'roller' phenotype

Table S2. Strains used in this study

Name	**Genotype**
N2	wild type
YY538	*hrde-1(tm1200*) III.
MT17463	*set-25(n5021)* III.
YY156	*nrde-2(gg95)* II.
BR3417	*spr-5(by134)* I.
RB995	*hpl-2(ok916)* III.
MT13293	*met-2(n4256)* III.
SS186	*mes-2(bn11) unc-4(e120)*/mnC1 *dpy-10(e128) unc-52(e444)*II.
JK2663	*dpy-11(e224) mes-4(bn67)* V/nT1 [*unc-?(n754) let-? qIs50*] (IV;V).
BCN1050	*unc-119(ed3)* III; *crgIs1002[daf-21p::mCherry::unc-54 3'UTR; unc-119(+)]*
BCN1049	*unc-119(ed3)* III; *crgIs1004[daf-21p::GFP::unc- 54 3'UTR; unc-119(+)]*
BCN1082	*crgIs1004[daf-21p::GFP::unc- 54 3'UTR; unc-119(+)];* single copy
TJ375	*gpIs1[hsp-16-2p::GFP]*
KM267	*pKM1211(hsp-16.41::hlh-1* + pRF4 *(rol-6))*
MH1870	*kuIs54[sur-5::gfp]*
CL2166	*dvIs19[pAF15(gst-4p::GFP::NLS)]*.
CF1553	*muIs84[pAD76(sod-3p::GFP)]*
SJ4005	*zcIs4[hsp-4p::GFP] V*

Table S3. Primers used for quantitative RT-PCR

Primer Pair	Forward Primer	Reverse Primer	Template	Targets
cec-1q	AGGAAGAGGAAGAAGAGGAG	CTGGTTCCACTATCGTAGTC	cDNA	*cec-1*
cdc-42q	GACAATTACGCCGTCACAG	CGTAATCTTCCTGTCCAGCA	cDNA	*cdc-42*
MIRAGE1q	CATTGTCAACTCAATGGTTCG	CCGACATTTTTCTCATGATGC	cDNA	WBTransposon00000001, WBTransposon00000002, WBTransposon00000003, WBTransposon00000004, WBTransposon00000005, WBTransposon00000006
CeMUDR1q	AGGTCGGCTAGAAATCGTACC	GTTCGATACCCCACAGATCAA	cDNA	WBTransposon00000610, WBTransposon00000633, WBTransposon00000647, WBTransposon00000722, WBTransposon00000723
GFPg	TGGAAGCGTTCAACTAGCAG	AAAGGGCAGATTGTGTGGAC	genomic DNA	*gfp*
cdc42g	CTGCTGGACAGGAAGATTACG	CTCGGACATTCTCGAATGAAG	genomic DNA	*cdc-42*
csq1g	AACTGAGGTTCTGACCGAGAAG	TACTGGTCAAGCTCTGAGTCGTC	genomic DNA	*csq-1*
MIRAGE1g	ACAATGGACTGGGCATGAGC	CGGAATGCAGCTTCGGTTTT	genomic DNA	WBTransposon00000001, WBTransposon00000002, WBTransposon00000003, WBTransposon00000004, WBTransposon00000005, WBTransposon00000006
CeMUDR1g	GCCACACTGGGAACTGAGAA	TGATTTCTCACGCAATGCACC	genomic DNA	WBTransposon00000610, WBTransposon00000633, WBTransposon00000647, WBTransposon00000722, WBTransposon00000723
MIRAGE1_7	GGGATCTTGGTTTGGGTTTAGG	TTTTCTGTCGCTCTGCCGTG	genomic DNA	WBTransposon00000002
MIRAGE1_51	TGCCGTATATTTACGCATTTACTGA	TTTTCTGTCGCTCTGCCGTG	genomic DNA	WBTransposon00000006
MIRAGE1_52	CCACCCAAGCACATAGATTCCA	TTTTCTGTCGCTCTGCCGTG	genomic DNA	WBTransposon00000001
MIRAGE1_45	CGATGTTCCCAAATTTTCAGGCT	TTTTCTGTCGCTCTGCCGTG	genomic DNA	WBTransposon00000003
CEMUDR1_67	GATGAGGCACCGTCTACCATC	TCAGTAGCGAAAAAGACACTCGT	genomic DNA	WBTransposon00000647
CEMUDR1_332	AGATTTTACAGCCACGTACGGTTC	CCATTTTCGTGCAAACACACATTC	genomic DNA	WBTransposon00000723
CEMUDR1_149	GTTTGCCTGTTTTGGAATAGGGT	AAGGCTACGGTGAGGTGCTG	genomic DNA	WBTransposon00000633

Table S4. Biological correlation between log2 expression fold change in *set-25* mutants and at high temperature (25°C).

Analysis of the RNA-seq data analyzed in Figure 4 but here analyzed using limma and the genas function (*35*). Briefly, this method estimates the correlation between log fold-changes in the three conditions (*set-25* mutant, high temperature and low temperature) if they could be measured without error. The estimated biological correlation of changes in expression of DNA transposons and several other repeat classes are positive and significant irrespective of the method used.

A. Expression data based only on uniquely mapping reads.

	Gene subset used for the calculation of biological correlation							
	p.union		Fpval		logFC		predFC	
	Biological Correlation	p.value	Biological Correlation	p.value	Biological Correlation	p.value	Biological Correlation	p.value
DNA transposons	0.86	2.00E-16	0.25	1.19E-05	0.51	2.00E-16	0.53	2.00E-16
Pseudogenes	0.34	1.42E-04	0.31	7.33E-04	0.49	8.64E-04	0.42	3.62E-03
Satellites	0.78	1.17E-05	0.26	1.32E-01	0.52	7.43E-04	0.51	5.18E-04
Rolling circle transposons	0.70	7.10E-05	0.40	8.98E-03	0.62	4.30E-05	0.56	8.39E-05
Other	1.00	1.54E-06	0.06	6.57E-01	0.51	4.91E-07	0.49	3.62E-07
Protein coding	0.13	2.00E-16	0.10	5.60E-16	0.13	9.41E-08	0.15	1.88E-13
LINEs & SINEs	0.13	7.00E-01	0.01	9.71E-01	0.28	5.30E-01	0.15	6.69E-01
LTRs	-0.20	2.97E-01	-0.30	1.04E-01	-0.53	3.00E-02	-0.34	2.01E-01

B. Expression data based on uniquely and multi-mapping reads.

	Gene subset used for the calculation of biological correlation							
	p.union		Fpval		logFC		predFC	
	Biological Correlation	p.value	Biological Correlation	p.value	Biological Correlation	p.value	Biological Correlation	p.value
DNA transposons	0.77	2.00E-16	0.46	2.00E-16	0.70	2.00E-16	0.61	2.00E-16
Pseudogenes	0.37	3.38E-06	0.33	3.98E-05	0.51	1.09E-04	0.45	6.56E-04
Satellites	0.46	3.85E-04	0.17	2.19E-01	0.51	2.76E-04	0.44	8.00E-04
Rolling circle transposons	0.81	6.94E-08	0.46	2.92E-04	0.67	1.24E-06	0.63	3.25E-07
Other	0.88	5.33E-08	0.21	9.48E-02	0.54	5.21E-08	0.52	1.59E-08
Protein coding	0.13	2.00E-16	0.09	2.80E-14	0.13	7.78E-09	0.15	8.36E-13
LINEs & SINEs	0.19	3.98E-01	-0.11	6.28E-01	0.31	3.03E-01	0.19	4.42E-01
LTRs	-0.39	8.86E-03	-0.42	4.27E-03	-0.58	8.72E-03	-0.41	7.06E-02

C. Expression data based on uniquely and multi-mapping reads. Here, all reads from repeats belonging to the same subfamily were combined into one value.

	Gene subset used for the calculation of biological correlation							
	p.union		Fpval		logFC		predFC	
	Biological Correlation	p.value	Biological Correlation	p.value	Biological Correlation	p.value	Biological Correlation	p.value
DNA transposons	0.72	1.69E-05	0.69	2.46E-05	0.83	1.18E-03	0.81	1.34E-03
Pseudogenes	0.36	4.13E-06	0.33	5.16E-05	0.52	8.37E-05	0.44	7.02E-04
Satellites	NA	NA	NA	NA	NA	NA	NA	NA
Rolling circle transposons	NA	NA	NA	NA	NA	NA	NA	NA
Other	NA	NA	NA	NA	NA	NA	NA	NA
Protein coding	0.12	2.00E-16	0.09	2.96E-13	0.14	1.44E-09	0.15	1.67E-13
LINEs & SINEs	NA	NA	NA	NA	NA	NA	NA	NA
LTRs	-0.52	2.17E-02	-0.53	1.54E-02	-0.88	7.62E-03	-0.76	4.18E-02

p.union: Genes that have a significant moderated t-test p.value in either comparison.
Fpval: Genes chosen based on how many F-test p-values are estimated to be truly significant.
logFC: Genes with log fold-change at least as large as the 90th percentile of the log fold-changes.
predFC: Genes with predictive log fold-change at least as large as the 90th percentile of predictive log fold-changes on the absolute scale.
NA: Not enough data to run the test.

References

27. T. Stiernagle, Maintenance of C. elegans. *WormBook : the online review of C. elegans biology*, 1-11 (2006).
28. A. Burga, M. O. Casanueva, B. Lehner, Predicting mutation outcome from early stochastic variation in genetic interaction partners. *Nature* **480**, 250-253 (2011).
29. C. J. Bean, C. E. Schaner, W. G. Kelly, Meiotic pairing and imprinted X chromatin assembly in Caenorhabditis elegans. *Nat Genet* **36**, 100-105 (2004).
30. D. S. Portman, Profiling C. elegans gene expression with DNA microarrays. *WormBook : the online review of C. elegans biology*, 1-11 (2006).
31. R. Brankatschk, N. Bodenhausen, J. Zeyer, H. Burgmann, Simple absolute quantification method correcting for quantitative PCR efficiency variations for microbial community samples. *Applied and environmental microbiology* **78**, 4481-4489 (2012).
32. D. Kim *et al.*, TopHat2: accurate alignment of transcriptomes in the presence of insertions, deletions and gene fusions. *Genome biology* **14**, R36 (2013).
33. Y. Liao, G. K. Smyth, W. Shi, featureCounts: an efficient general purpose program for assigning sequence reads to genomic features. *Bioinformatics (Oxford, England)* **30**, 923-930 (2014).
34. M. I. Love, W. Huber, S. Anders, Moderated estimation of fold change and dispersion for RNA-seq data with DESeq2. *Genome biology* **15**, 550 (2014).
35. M. E. Ritchie *et al.*, limma powers differential expression analyses for RNA-sequencing and microarray studies. *Nucleic acids research* **43**, e47 (2015).